Running Title: ACTIVITY AND DENDRITIC ARBORIZATION

Unilateral Primary Afferent Nerve Cut Causes Altered Pruning of Dendrites in the Developing Central Taste System

A Thesis Presented to the Faculty of the Neuroscience Program

By David J. Doobin

Washington and Lee University

Neuroscience Program

16 May 2011

Acknowledgements

I would like to thank my supervisor, Dr. Robert Stewart, who provided the guidance, direction, and motivation to complete this body of work. I am also indebted to the members of the Stewart lab who helped with this project: Beverly Bowering, the skilled lab technician who taught me many techniques and supervised the laboratory; Dr. Sarah Blythe, who helped with Golgi-staining techniques; and Maddin Nelson and Nicole Herbst, who assisted me in animal care.

None of this would have been possible without Dr. Peter Brunjes and Dr. David Hill, who provided us with the Golgi solution and staining assistance, as well as generously letting us use the microscopy equipment in their lab. Thank you to Dr. Jack Weilgus and Dr. Wade Bell, who were both patient readers on my thesis committee and provided remarkable insight. I am deeply grateful to Dr. Tyler Lorig for his advising and mentorship over the past four years, and Dr. Len Jarrard for his research advice and wisdom. T the faculty at Washington and Lee University and Newark Academy – thank you for developing my intellect and character beyond what I ever imagined I was capable of.

Finally, thank you to my friends and family for their support through this point and forward.

Abstract

The development of the taste system mirrors that of other sensory systems, and thus an understanding of gustatory developmental phenomena can provide insight into developmental processes in general. Changes in taste stimulus-driven activity during gustatory development are dynamic: step-wise maturation of taste buds, age-related alterations in taste primary afferent nerve responsiveness, and alterations in patterns of synaptic connections in the nucleus of the solitary tract all occur during a protracted postnatal period. We hypothesized that these structural and functional changes help to shape the dendritic morphology of the neurons located in the nucleus of the solitary tract (NTS), the sole site of peripheral taste sensory input, specifically by reducing the complexity of these dendritic arbors, i.e., that dendritic 'pruning' occurs in response to patterned taste activity. This was investigated by unilaterally cutting the lingual tonsilar branch of the glossopharyngeal nerve – which projects to the NTS – in 18 day old hamsters and using Golgi-Cox staining to examine dendritic morphology of NTS neurons at three post nerve-cut survival times. NTS neurons were traced and dendritic segment length was analyzed along with dendritic node quantity and cell body area for two defined classes of neurons in the NTS. It was found that animals in the shortest survival time group (31 days post-nerve cut, or 49 days-old) had neurons with significantly longer dendritic branch lengths, more dendritic branch nodes, and increased cell body area in the NTS ipsilateral to glossopharyngeal nerve cut. This effect disappeared when animals were allowed to survive 65 days following nerve cut. (83 days-old). This result suggests that the loss of afferent input induces a reversible delay in normal dendritic pruning. We speculate that delayed pruning may occur consequent to axonal sprouting and rearrangement of the terminal

fields of the remaining two major taste nerves. This would compensate for the lack of afferent synaptic activity and initiate late stage pruning of the dendritic arbors.

INTRODUCTION

Anatomical and Physiological Overview of the Mammalian Taste System

The most basic units of taste stimulus detection are taste-receptor cells (TRCs), which are located throughout the oropharynx, but most prominently on the dorsal epithelium of the tongue and in the palate (Chandrashekar et al., 2006). Lingual and palatal TRCs are aggregated into taste buds. As noted below, lingual taste buds are embedded within specialized epithelial papillae, while those in the palate are found within the oral epithelium proper. Taste buds consist of numerous (50-150) TRCs clustered around a centrally located taste pore, which is the site of interaction between TRC apical villi and taste stimuli.

TRCs possess two functionally distinct membrane domains, apical and basolateral. The apical domain includes microvilli which contact the oral milieu via the taste pore and contain receptor elements for detection of taste stimuli (Chandrashekar et al., 2006). The basolateral domain, which is located below the tight junctions that connect the TRCs near their apices, contains ion channels that permit action potentials to be conducted and synaptic transmission to occur between TRCs and associated gustatory primary afferent axons. Primary afferent axons enter the ventral part of the taste bud before ramifying within it (Chandrashekar et al., 2006).

There are three types of lingual taste papillae found in mammals (Figure 1A). The first type is circumvallate papillae, which are located on the posterior tongue and contain hundreds of taste buds. In rodents there is typically a single, midline circumvallate papillae, while other mammals tend to have several circumvallate arranged symmetrically across the lingual midline. The circumvallate papilla consists of a semicircular invagination

yielding a semicircular trench, the walls of which are studded with hundreds of taste buds (Chandrashekar et al., 2006). These papillae are innervated by the lingual-tonsilar branch of the glossopharyngeal nerve (IXth cranial nerve) (May & Hill, 2006).

Foliate papillae are found on the posterior-lateral sides of the tongue and contain ten to a few hundred taste buds, depending on the species. Foliate papillae comprise several invaginations of epithelium, with the walls of the resulting vertically-oriented grooves lined with several hundred taste buds (Chandrashekar et al., 2006). The taste buds in the anterior grooves of the foliate papillae are innervated by the chorda tympani (CT) branch of the facial nerve (cranial nerve VII) nerve, while those in more posterior grooves are innervated by the IXth cranial nerve (May & Hill, 2006).

Fungiform papillae are located in the anterior dorsal lingual epithelium and generally contain one or a few taste buds, again depending on the species (Chandrashekar et al., 2006). Fungiform papillae number in the hundreds and receive afferent innervation by the CT (May & Hill, 2006). Another branch of the facial nerve, the greater superficial petrosal nerve (GSP), innervates palatal taste buds (May & Hill, 2006). Palatal taste buds are found in the nasoincisal papilla, on the border between the hard and soft palate, and throughout the soft palate (Chandrashekar et al., 2006). Palatal taste buds outside of the nasoincisal papilla are not located in discrete papillae, but rather in the mucosal wall proper (Chandrashekar et al., 2006). Finally, laryngeal taste buds are solitary structures found in the mucosa of the oropharynx and epiglottal folds of the posterior oral cavity (Miller & Smith, 1984). Laryngeal taste buds are innervated by the superior laryngeal branch of the vagus nerve (cranial nerve X) (Miller & Smith, 1984). All of these taste buds

and their projections are displayed graphically in Figure 1A (adapted from Mangold & Hill, 2008).

Anatomy of Primary Afferent Taste Axons & Their Projections

The axons that convey gustatory information to the CNS all exit at the base of the taste buds and project to the nucleus of the solitary tract (NTS) (Hill & May, 2007), a major sensory relay nucleus located in the dorsal medulla (King, 2007). Cell bodies of axons of CT and GSP nerves reside in the geniculate ganglion and project axons to the rostral pole of the NTS (May & Hill, 2006). Cell bodies of the lingual-tonsilar branch of the IXth nerve reside in the petrosal ganglion, and project axons to both the rostral NTS and the caudal NTS (Travers & Norgren, 1995). It is thought that only the projection to the rostral pole is involved in taste special sensory processing, while the caudal projection serves general visceral sensory roles (Travers & Norgren, 1995). The superior laryngeal branch of the IXth nerve, which has cell bodies in the nodose ganglion, projects axons to the intermediate NTS (Miller & Smith, 1984). The superior laryngeal branch of the IXth nerve plays a more significant role in oromotor reflex initiation than in taste sensation and perception (Stewart & Hill, 1993).

Taste neurons in the NTS project taste information via three functionally distinct pathways – the sensory-discriminative pathway, the affective pathway, and the oromotor pathway (Travers & Norgren, 1995). The sensory discriminative pathway involves taste information from the primary afferent nerves passing synaptically through the NTS, from where it continues on an ascending pathway to the parabrachial nucleus (PBN) in the pons (Fulwiler & Saper, 1984). From PBN most taste information is projected to the ventral posteromedial thalamus, and these thalamic neurons, in turn, project axons to the insular

cortex (Wolf, 1968). A sparser ascending pathway – the so-called affective pathway – projects from the PBN to the ventral forebrain, lateral hypothalamus, and finally to the central nucleus of the amygdala (Norgren, 1974; Norgren, 1976; Bernard, Alden, & Besson, 1993). Together, these pathways are responsible for the perception of tastes and the hedonic behaviors that accompany them; for example the conditioning people undergo such that normally aversive tastes become attractive (King, 2007).

The oromotor pathway projects from the NTS to the oromotor nuclei of the reticular formation (Streefland & Jansen, 1999). Axons in this pathway, which is also known as the descending output pathway, project from the NTS to medullary oromotor nuclei in the parvocellular reticular formation (Norgren, 1995). The descending pathway also has axons that terminate in the salivatory nuclei and brainstem oromotor nuclei. This pathway is responsible for commonly seen rejection behaviors, which occur almost immediately in the presence of aversive taste stimuli (King, 2007), but it does not play a major role in taste sensation and perception.

Descending Inputs to Gustatory Pathways

There are also descending inputs into the NTS that originate in several brain regions, including the brainstem and forebrain (King, 2007). Inputs from the brainstem include the parabrachial nucleus, which is thought to alter gustatory information processing by modulating both ascending and descending output from the NTS (Whitehead, Bergula, & Holliday, 2000; Karimnamazi & Travers 1998). Forebrain projections from the insular cortex and amygdala also alter gustatory information processing by affecting ascending and descending output (King, 2007). For example, projections from the insular cortex have been shown to alter the processing of information

within the NTS itself and to modulate information leaving the NTS (Smith & Li, 2000). Descending inputs from amygdala are dense in areas of the NTS that project to the oromotor nuclei, suggesting that they modulate oromotor behavior responses (Halsell, 1998; Li, Cho, Smith 2002). A simplified schematic of both ascending and descending gustatory pathways is depicted in Figure 1b (Roper 2009).

Peripheral Taste Function

The stimulus sensitivity of individual taste axons varies by species as well as by location in the oral cavity (Davis et al., 2000), although certain trends are evident. In the mammalian order, most individual taste axons show multimodal sensitivity (Travers & Norgren, 1995). This most likely reflects the fact that individual taste axons sample multiple taste receptor cells synaptically, and thus integrate taste information from multiple taste cells at once. This observation renders the common textbook depiction of an "oral taste map" incorrect (Chardrashekar et al., 2006).

In rodents, taste receptor cells innervated by the CT appear most sensitive to salts, acids, and sugars, and less sensitive to compounds that are rejected behaviorally and perceived as bitter by humans (Smith & Davis, 2000). Likewise, neural recordings from rat (Nejad, 1986; Sollars & Hill, 2005) and hamster (Harada & Smith, 1992) indicate that taste receptor cells innervated by the GSP are highly sensitive to sugars and salts, while not as sensitive to bitter or sour taste stimuli. In contrast, taste receptors innervated by the IXth nerve are relatively more sensitive to bitter and sour than to sweet or salty stimuli (Smith & Davis, 2000). It may be that this pattern of stimulus sensitivity reflects unequal regional oropharyngeal distribution of transduction pathway components, although this has yet to be established conclusively (Chandrashekar et al., 2006; Stewart & Hill, 1993).

Gustatory Transduction Pathways

The current view is that five different taste modalities (i.e., sweet, umami, bitter, salty, and sour) are detected by different, specialized receptors on TRC apical membranes. The T1Rs comprise a family of three homologous of G-protein-coupled receptors (T1R1, T1R2, and T1R3) that associate in various ways to create unique sweet and umami taste receptors (Nelson et al., 2001). Functional sweet taste receptors are thought to be a heterodimer composed of T1R2 and T1R3 (Nelson et al., 2001). The receptor complexes are characterized by long amino-terminal extracellular domains, which mediate taste stimulus recognition and binding (Kunishima, 2000). These dimeric receptors bind with and initiate transduction cascades for all sweet taste stimuli, which include natural and artificial sugars, some D-amino acids, and several intensely sweet proteins (Nelson et al., 2001).

Umami taste, which is associated with foods rich in L-amino acids, is highly attractive to most mammals (Zhao et al., 2003). Umami taste receptors comprise a T1R1/T1R3 heterodimer (Nelson et al., 2002). Thus, the receptor complexes for both sweet and umami stimuli contain T1R3. While taste stimuli for umami receptors include many L-amino acids across species, in humans only two – monosodium glutamate (MSG) and aspartate – evoke umami sensations (Zhao et al., 2003). Umami tastants have also been shown to suppress weight gain and reduce plasma leptin levels in rats, possibly through the activation of glutamate receptors within the gastrointestinal tract (Kondoh & Toril, 2008).

While the T1R heterodimeric receptors for umami and sweet stimuli appear to be responsible for detection of all structurally-related stimuli within each submodality, taste

receptor cells that are sensitive to bitter stimuli are responsible for detecting a wide range of structurally dissimilar, typically toxic compounds, (Chandrashekar, 2006). Perhaps not surprisingly, bitter taste receptors comprise a family of approximately 30 moderately homologous G-protein-coupled receptors called T2Rs (Alder et al., 2000). The genes for T2Rs are selectively expressed in TRCs distinct from TRCs that express sweet or umami receptors. These TRCs also tend to express most – if not all – T2R genes, and hence are tuned to a wide variety of bitter taste stimuli (Alder et al., 2000). It also appears to be the case that T2R-expressing TRCs are most numerous in taste buds within the circumvallate and foliate papillae, while those that bear T1Rs are most common in taste buds on the anterior tongue. (Nelson et al., 2001)

Salty and sour taste are often discussed together because both are thought to involve the direct entry of cations into the TRCs via specialized membrane channels located on the TRC apical surface (Chandrashekar, 2006). For salty taste, Na^+ and other, mostly monovalent cations, are transduced via amiloride-senstive Na^+ channels,(Heck, Mierson, DeSimone, 1984), as well as via vanilloid receptor type 1 channels (Lyall et al., 2004). Sour stimuli are believed to be detected by PKD2L1 ion channel receptors, which allow H^+ cations to pass (Huang et al., 2006), and hence sour taste is a response evoked by acids (DeSimone & Lyall, 2006). PKD2L1 receptors are also found in other areas of the body where they help to sense H^+ and pH levels, such as monitoring CO_2 levels in the blood and proton levels in cerebrospinal fluid (Huang et al., 2006).

This brief overview of gustatory structure and function serves to illustrate the diverse array of structural and functional loci that must undergo maturation during development of the taste system. In the following sections, we discuss how in some species

substantial anatomical and physiological maturation of the taste system occurs *ex utero*. We argue that these trends could represent the basis for large, dynamic changes in taste stimulus-driven neural activity that, in turn, may have a role in shaping the synaptic connectivity of the mature gustatory system.

Gustatory Development

The development of the peripheral taste system has been more extensively studied than that of the central taste system, although even the literature on peripheral taste development remains small (Stewart, DeSimone, & Hill, 1997). Information on the morphological development of the peripheral taste system is much more abundant than information on its functional development. For example, it has been shown that appearance and anatomical maturation of taste buds depends on their oropharyngeal location. Hence taste buds in the fungiform, foliate, and circumvallate papillae, as well as the soft palate mature at different times in both rats (Harada et al, 2000) and hamsters (Belecky & Smith, 1990). There are also notable trends in functional development that may reflect both anatomical maturation and the appearance of receptor mechanisms for various taste modalities. A useful feature of peripheral taste functional development is that it can be used to predict changes in central taste system neurophysiology and developing taste-related behaviors (Stewart & Hill, 1993).

Development of Taste Buds

The development of taste buds and hence TRCs varies across mammalian species, occurring prenatally for those with long gestation periods such as humans, monkeys, cats, and sheep. In species with shorter gestation periods, however, such as rodents, taste bud development occurs postnatally (Belecky & Smith, 1990). For example, in hamsters, taste

buds in the foliate and circumvallate papillae are absent at birth and develop over the first three months of life (Miller & Smith, 1988). In rats, fungiform papillae and soft palate taste buds are present at birth, but they are highly immature (Mistretta 1972), and some studies have even suggested that the development of rat palatal taste buds occurs entirely postnatally (Srivastava & Vyas, 1979).

Development of functional TRCs may be important in development of the central gustatory system because TRCs may provide a source of patterned activity that helps shape the mature central gustatory system. Focusing on the hamster, taste buds located in different regions of the oropharynx mature at different points postnatally, and generally in a rostral to caudal gradient. As noted, taste buds in the circumvallate and foliate papillae are absent at birth, but between birth and the first 10 days of life there is a large increase in the number of taste buds in these structures (Miller & Smith, 1988). The rapid proliferation of taste buds anticipates the weaning of the hamsters, which occurs at approximately 3 weeks of age. Foliate papillae taste buds continue to develop until reaching an adult-like number around 2 months of age, while the taste buds in the circumvallate papillae continue to increase in number until as late as 4 months of age (Miller & Smith, 1988).

Contrary to the taste buds of the foliate and circumvallate papillae, soft palate taste buds in the hamster are present in near adult numbers at birth, although only 39% of these are morphologically mature, that is they have open taste pores (Belecky & Smith, 1990). These palatal taste buds are localized mostly to the posterior and medial portions of the soft palate and undergo maturation to adult form during the first 20-30 days of postnatal life (Belecky & Smith, 1990). Fungiform papillae taste buds undergo extensive maturation

during embryonic development, and are present in adult number and form shortly after parturition (Whitehead & Kachele, 1994). Finally, taste buds located on the laryngeal surface of the epiglottis and the aryepiglottal folds are absent at birth. These taste buds, which are innervated by the vagus nerve, appear and mature over the first 120 days of development.

This striking, protracted postnatal appearance and maturation of taste buds is likely to engender significant, stimulus-dependent alterations in taste primary afferent activity during the same period. Given the clear role of patterned activity in the development and maturation of other neural systems (Ruthazer and Aizenmen, 2010), it is tempting to speculate that the combined anatomical and physiological development of the peripheral taste system act together to shape development of the central taste system in hamsters.

Sweet Taste Development

Although it took researchers longer to discover how sweet taste receptors function compared to the other taste modalities, ultimately resulting in the discovery of the heterodimeric T1R G-protein coupled receptors (Nelson et al., 2001), the development of sweet taste function has indeed been investigated. Hill (1988) did extensive work examining sweet taste responses in the CT nerve of developing hamsters. He found that developing hamsters showed different developmental patterns in CT responses to monosaccharide sugars compared to disaccharide sugars. With regard to the monosaccharide sugars fructose and glucose, CT responses were significantly smaller in pre-weanling hamsters (14-20 days old), and CT responses of recently weaned hamsters (25-35 days old) were of magnitudes intermediate to those in preweanling and adult hamsters.

While monosaccharide responses of the chorda tympani demonstrated a gradual increase during postnatal development, disaccharide sugars displayed a different trend. Hamster CT responses to the monosaccharide sugars reached a mature level at 25-35 days, while the disaccharide sugars did not elicit mature responses until after this time period (Hill, 1988). These results suggest that in hamsters development of CT sensitivity to monosaccharide and disaccharide sugars occurs at different rates, with maturation occurring earlier for simpler monosaccharide sugars compared to more complex disaccharide sugars (Hill, 1988).

Harada and Maeda (2004) demonstrated a different pattern of sweet taste development in rats, however. Recordings of CT responses revealed no differences in response magnitudes between monosaccharide sugars D-fructose, D-glucose, and D-galactose and disaccharide sugars sucrose, lactose, and maltose. Instead, their recordings showed that responses to sucrose increased during 1-3 weeks of development, reached a maximum, and then decreased until 8 weeks after birth. CT responses to other sugars studied tended to follow a similar pattern of development, as seen in Figure 2. The direction of this developmental trend is opposite to that observed for saccaharide responses in hamster CT. The decrease in sugar-elicited CT response magnitudes between about 2 to 8 weeks of age is hypothesized to result from a decrease in the number of sweet or sucrose sensitive fibers in the CT, or in the number of sucrose sensitive receptor sites on the TRCs within taste buds (Harada & Maeda, 2004).

Salt Taste Development

Much of the research done on the development of salt taste function has concerned chorda tympani responses to NaCl and LiCl in mouse (Ninomiya et al., 1991), sheep

(Bradley & Mistretta, 1973), hamster (Hill, 1988), and rat (Hill & Bour, 1985). Early work in sheep, by Bradley and Mistretta (1973), indicated that CT responses to NaCl and LiCl increased with age in lambs, while responses to KCl decreased with age. The developmental changes seen by Bradley and Mistretta have more recently been attributed to an increase in the functional expression of amiloride-sensitive Na^+ channels in the apical membranes of developing sheep taste receptor cells (Stewart and Hill, 1993).

Data from mouse and rat models also show that chorda tympani sensitivity to NaCl (and LiCl) increases with age (Hill & Amli, 1980; Yamada, 1980; Ninomiya et al., 1991). In rat, a dramatic increase in Na^+ and Li^+-stimulated CT responses occurs between birth and about 60 days of age, at which point the responses reach unchanging, mature levels. The developmental change in CT responses to NaCl and LiCl in rats is believed to be due to increases in single fiber sensitivity, specifically to these salts (Hill, Mistretta, & Bradley, 1982). Because increases in CT sensitivity to NaCl and LiCl in rats occur concurrently with increasing gustatory susceptibility to amiloride inhibition of responses to these salts, the mechanistic basis for this developmental change may be the addition of functional epithelial Na^+ channels to TRC apical membranes (Hill & Bour, 1985).

While rat and sheep demonstrate developmental increases in chorda tympani Na^+ sensitivity, Hill (1988) reported that salt taste development in hamsters follows a very different path. In hamster, CT responses to LiCl and NaCl *decreased* between about 15 days of age and adulthood. Moreover, CT responses to Na^+ were amiloride-sensitive in hamsters as young as 7 to 9 days old (Hill, 1988). These results reveal a strikingly different pattern in salt taste development compared to rat, although it should be noted that the conclusions are based on methods using whole nerve relative response data. This leaves open the

possibility that age-related increases in CT responses to the NH_4Cl reference stimulus could account for the apparent decrease in responses to Na^+ sensitivity (Stewart, DeSimone, Hill, 1997).

Bitter, Sour, and Umami Taste Development

There is a dearth of literature that describes functional development of bitter, sour, and umami taste modalities. Of the three, the bitter taste modality is probably the best understood, since a handful of studies have examined the onset of CT responses to quinine in rats (Yamada, 1980) as well as in mice (Ninomiya et al., 1991). Results from rats show an age-related decrease in magnitude of CT responses to quinine (Yamada, 1980). These results remain questionable, however, because nerve responses to quinine were measured as a ratio of adult responses to a 0.1M NaCl standard stimulus solution. Hence the apparent age-related decrease in quinine sensitivity may be due to previously described increases in CT Na^+ responses (Hill & Amli, 1980; Stewart & Hill, 1993). Studies examining glossopharyngeal responses in mice have shown different response patterns than those in rats, with an apparent age-related increase in responses to quinine (Ninomiya et al., 1991). This increase in sensitivity may be due to an increase in the number of taste buds that contribute to the whole glossopharyngeal nerve response (Stewart & Hill, 1993). Finally, preliminary results from our lab reveal an age-related biphasic change in hamster CT sensitivity to quinine. Specifically, CT response magnitudes to quinine increase between 14 and 21 days of age and then decrease to mature, unchanging values by about 45 days of age (R. Stewart, unpublished results). This curious developmental pattern may function to make the organism maximally sensitive to toxic ingesta at a time when it is beginning to

engage in free-feeding. Transiently elevated peripheral sensitivity might also allow weanling hamsters to learn efficiently to avoid specific tastes associated with toxicity.

While there is substantial interspecific variability in peripheral gustatory functional development, a common theme is that peripheral sensitivity to major taste stimuli varies, sometimes dramatically, during early postnatal life in several altricial rodent species. Moreover, remarkable and oppositely directed alterations in stimulus sensitivity can occur on unique time courses in the same afferent nerve. For reasons of surgical convenience, most developmental changes in gustatory stimulus sensing have been observed in the CT. It seems reasonable to expect that parallel changes in GSP and IXth nerve stimulus sensitivities also occur. Together, with known postnatal development of taste buds, these functional changes constitute remarkably dynamic fluctuation of stimulus-generated afferent neural activity that extends in rat and hamster nearly to the onset of sexual maturity.

Central Gustatory Development

Research into the functional development of central gustatory pathways lags behind that concerning the peripheral gustatory system, although peripheral development research has been used to predict changes in central taste system neurophysiology (Stewart & Hill, 1993). Two major studies have examined taste functional development in the CNS: one investigated development in the rat NTS (Hill, Bradley, Mistretta, 1983) and the other focused on the rat PBN (Hill, 1987).

Functional Development of the NTS

In rats, multiunit responses from the NTS in the first postnatal week indicate that NST neurons aged 5 to 7 days respond to NH_4Cl, KCl, HCl, and citric acid at high

concentrations (0.5M) (Hill, Bradley, Mistretta, 1983). These same neurons failed to respond to NaCl, suggesting a lack of functional transduction elements for Na^+ at this age (Stewart & Hill, 1993). It was also shown in rat that NTS responses to aversive and toxic taste stimuli are mature at an early age (Scott & Mark, 1987), while responsiveness to taste stimuli with associated nutritional value increases monotonically with age. The developmental changes in the NTS temporarily parallel those observed in the CT to a certain extent (Stewart & Hill, 1993).

Differences between CT and NTS neurophysiological development include stimulus specificity, such that the peripheral gustatory system exhibits developmental changes in stimulus specificity that are largely absent in the NTS (Stewart & Hill, 1993). It has also been shown that in sheep NTS neurons fail to respond to NaCl and LiCl at early stages of postnatal development, even though the peripheral receptors for these salt stimuli are functional (Bradley & Mistretta, 1980). With advancing age, axons from the CT increasingly converge on individual target neurons in NTS, which is thought to result in the emergence of Na^+ sensitivity. This result also implies that refinements of synaptic relationships between taste afferent axons and NTS target neurons gives rise to mature neurophysiological functions in NTS (Stewart & Hill, 1993).

Functional Development of the PBN

PBN neurons also exhibit major developmental changes, with PBN neurons in rats at ages 4-7 days responding to most, but not all, stimuli (Hill, 1987). By 14 days of age, neurons in the rat PBN respond to all stimuli tested. This indicates that rat PBN neurons mature completely between the first and second week of development (Hill, 1987). Interestingly, this pattern precedes the functional maturation of the peripheral gustatory

system. However, after 14 days of age, response frequencies to all stimuli continue to increase to mature levels, which suggests that there is significant, ongoing convergence of NTS inputs onto PBN neurons as the NTS continues to mature (Stewart & Hill, 1993). Taken together, data concerning the functional development of NTS and PBN neurons strongly imply that maturation of synaptic relationships between pre- and postsynaptic elements occurs progressively during the postnatal period, and that these processes may rely in part on changes in stimulus-driven activity that arise in the periphery.

Anatomical Development of the NTS

Of the three cranial nerve branches that provide taste input to the NTS, the development of CT and IXth nerve inputs have been most extensively studied (Lasiter, Wong, Kachele, 1989; Lasiter, 1992). In rat CT axons begin to synapse in NTS beginning at postnatal day 1, although the organization of the terminal field is not complete until P25 (Lasiter, 1992). In contrast, axons of the IXth nerve initially synapse in NTS beginning on postnatal day 10 and continue to expand into the intermediate NTS until about 45 days of age. Overlap of the terminal fields of the CT and IXth nerve is first observed around P10 and is maximal by 20 days of age (Lasiter, 1992). These results indicate that the terminal fields within the NTS develop on unique time courses.

In rat, NTS neurons are present beginning at E12, reach peak proliferation at E13, and have attained a maximum population by E16 (Altman & Bayer, 1980). Between postnatal days 4 and 20, first order dendrites of fusiform, multipolar, and ovoid NTS neurons grow rapidly. Signs of rapid growth of first order dendrites include increases in the activity of metabolic markers such as cytochrome oxidase, succinate dehydrogenase, and NADH. By 25 days of age, first order dendrites have reached adult length, while second

order dendrites of multipolar neurons continue to develop until 70 days of age (Altman & Bayer, 1990). The dendritic growth patterns of NTS neurons occur in parallel with dendritic development of PBN neurons (Lasiter & Kachele, 1988).

Axonal Terminal Field Development

The development of primary axonal terminal fields afferent to the NTS is of particular importance to the development of the NTS neurons themselves (Hill & May, 2007). CT axon terminal field growth occurs in two phases. The first phase involves expansion into the NTS between postnatal days 1 and 25 (Hill & May, 2007). At this point the terminal field begins to reduce in size. Between 25-27 and 35-37 days of age, CT terminal field volume decreases dramatically and then continues to decrease at a slower rate until adulthood (Sollars et al., 2006). This remodeling of the CT terminal field occurs in a temporal fashion that echoes parallel changes in CT taste response profiles. Sollars et al. (2006) also demonstrated that when terminal field pruning does not occur properly – due to insufficient sodium levels in the diet – taste-guided behavioral response maturation is also altered.

Examples from other sensory systems demonstrate that neuronal activity helps to shape axonal terminal fields (Hill & May, 2007). Extensive studies by O'Leary and colleagues (Stanfield & O'Leary, 1985; O'Leary & Stanfield, 1989; O'Leary et al., 1990) have demonstrated that extensive pruning of axonal terminal fields occurs during development of layer 5 neurons in the visual and motor cortices in responses to increased neural activity. A proposed mechanism for terminal field pruning in mammalian brains involves the recruitment of semaphorins in pyramidal axon branches, which can induce retraction of axon branches over distances of many millimeters (Bagri et al., 2003). Increased

neuronal activity provides an attractive explanation for CT terminal field pruning, since it has also been shown that there is a correlation between CT nerve neurphysiological responses and terminal field volume reduction (Sollars et al., 2006).

Others have examined development of all three taste nerve terminal fields and found similar patterns of axonal pruning (Mangold & Hill, 2007). For example, Mangold & Hill (2008) obtained results similar to those reported by Sollars et al. (2006), namely that CT axonal terminal field volume decreased substantially under normal developmental conditions (i.e., sodium replete chow). Moreover, they showed that terminal field volumes of both GSP and IXth decline dramatically (by up to 75%) between 15 and 35 days postnatally, at which time stable, mature terminal fields volumes are achieved. They attribute the changes in field volumes to terminal arbor pruning driven by afferent nerve activity.

Recently, our lab has presented preliminary data that show similar reductions in taste primary afferent nerve terminal field volumes in developing hamster NTS (Reidy et al., 2008). Specifically, terminal field volumes of CT and IXth nerve declined by up to 70% between 45 and 180 days of age. Thus, the developing hamster taste CNS undergoes major reorganization at the level of the first central taste relay. The pattern of developmental change is reminiscent of that observed in rat NTS, but it may occur comparatively later in the postnatal period.

Dendritic Arbor Development

The previous sections have detailed findings that describe anatomical and physiological bases for dynamic changes in stimulus-generated afferent activity in the developing taste systems of rat and hamster. In addition, tract tracing methods have

provided data that are consistent with the hypothesis that in these species taste axonal inputs to the NTS are subject to activity-dependent reorganization during at least the first several weeks of postnatal life. The degree of reorganization, as inferred from reductions in taste afferent axon terminal field volumes, is striking in its magnitude. Abundant previous work done by O'Leary and colleagues (Stanfield & O'Leary, 1985; O'Leary & Stanfield, 1989; O'Leary et al., 1990), among others, provides compelling evidence that patterned neural activity is responsible for the pruning of axonal arbors and terminal fields that results in high precision synaptic contacts in the mature nervous system.

Neural activity is likely to play a role in development of NTS neuron dendritic arbors as well, which is the focus of this paper. Indeed, NTS neurons connected both directly and indirectly with primary afferents would be expected to encounter major changes in synaptically-driven activity as 1) populations of taste receptors become functional; 2) as stimulus sensitivity alters within an afferent channel; and 3) as some synaptic inputs are pruned at the same time that others are strengthened and stabilized. In order to fully understand how changes in patterned-stimulus activity in the NTS might affect dendritic arborization, the process of dendritic arbor growth must be analyzed and correlated with known trends in peripheral gustatory development. The next section provides background on dendritic arbor development, which is then applied to expected changes in stimulus-dependent activity in the NTS to form a hypothesis that predicts changes in dendritic arbor morphology.

The Dependence of Dendritic Arbor Development on Synaptic Activity

Dendrites are the primary site of synaptic connection for input neurons, and thus the structure of the dendrite determines how the neuron will respond to synaptic input and

develop further (Cline, 2001). *In vivo* models have demonstrated that synaptic activity is integral to the development of dendritic arbors (Katz & Shatz, 1996; Cline, 2001; Shen et al., 2009). During early stages of brain development synaptic activity enhances dendritic arbor elaboration and growth, while during later stages synaptic activity stabilizes dendritic arbor structure (Cline, 2001). It has been hypothesized that the difference in the role of synaptic activity on dendritic arborization during early versus late development is due to alterations in the spatiotemporal expression of integral components of the signal transduction pathways influenced by increased synaptic activity (Cline, 2001).

There are different sources and patterns of neuronal activity in the developing brain, and these sources can change as brain development proceeds. The first type of activity arises from waves of action potentials produced by the developing retina, hippocampus, cortex, and spinal cord (Feller 1999). These waves of neural activity provide synaptic stimulation to both the neurons directly receiving the synaptic input as well as the postsynaptic partners of those neurons. A second type of neural activity is spontaneous and occurs only during restricted periods of development in cells located adjacent to one another (Yuste et al., 1995). This coordinated spontaneous activity is mediated by gap junctions, which is made evident by its continued presence even after the Na^+ channel antagonist tetrododoxin (TTX) is applied.

The third source of activity comes from the subplate of the developing cortex. The cortical subplate is a transient group of neurons in the neocortex of mammals that serves as a relay target of thalamic afferents (Shatz 1996). Subplate neurons extend axons into the developing cortical plate and modulate synaptic input. The fourth type of activity is driven by sensory and motor inputs (Katz & Shatz, 1996), which early in development is

related to spontaneous activity in the developing spinal cord caused by specific cellular mechanisms (Milner & Landmesser 1999). Each of these four types of activity affect distinct stages of brain development, with spontaneous, coordinated activity driving processes earlier and stimulus-driven, patterned activity driving later events, such as the role that sensory input plays in the fine-tuning of circuits within the visual system (Weliky & Katz, 1997).

Dendritic Arbor Development **in vivo**

With the advent of modern imaging techniques it is now possible to examine dendritic arbor growth in intact animal models, in particular the albino *Xenopus* tadpole (Rajan & Cline, 1998; Shen et al., 2009). Developing neurons typically extend an axon first and then after a delay of a few hours begin to elaborate the dendritic arbor. Dendritic arbor growth proceeds at a rapid pace, as measured by total dendritic branch length. After a couple days of rapid growth the arbor growth rate largely slows down, and the structure of the arbor changes less, as seen in Figure 3 (Wu et al., 1999).

While the growth of the dendritic arbor is often measured in branch length, as in Figure 3(b), another common method of measuring growth is to measure branch dynamics. Developing dendrites demonstrate a very high rate of branch dynamics, with the rate of branch additions and retractions nearly equal (Rajan & Cline, 1998). At first this seemed paradoxical since an equal rate of branch addition and retraction would mean that no new branches are formed cumulatively. Time lapsed images demonstrate, however, that dendritic arbor growth occurs through gradual increases in branch number and lengthening of existing branches (Shen, 2009). This is the same pattern of growth that presynaptic axons undergo during development. That is, branch dynamics appear to

function as a mechanism by which developing dendrites and axons test the environment before permanently placing an axon or dendrite there (Cline, 2001).

Another surprising finding was that the rates of branch additions and retractions decreased as neurons matured, suggesting diminished branch dynamics with increasing age and complexity of the neuron (Cline, 2001). Specifically, more complex neurons had rates of branch addition and retraction that were about half of those of the simpler neurons (Wu et al., 1999). Also, in more complex neurons the branch additions and retractions that occurred were limited to the terminal branch tips. Thus, the overall growth of the dendritic arbor was largely diminished since the additions and retractions were occurring over a much smaller spatial region (Cline, 2001).

Role of Synaptic Activity in Enhancing Dendritic Arbor Growth

Synaptic activity has been shown to regulate dendritic arbor growth (Katz & Shatz, 1996; Rajan & Cline, 1998; Cline, 2001; Shen, 2009), although the specific manner in which synaptic activity affects dendritic arbor growth depends on the stage of maturation of the neuron under study (Cline, 2001). One of the ways that synaptic activity influences dendritic arbor growth is through glutamatergic synaptic inputs (Wu, Malinow, & Cline, 1996). In *Xenopus* optic tectal neurons, dendritic arbor growth begins roughly when the neuron first receives glutamatergic retinotectal synaptic input (Cline, 2001). It has also been shown that NMDA receptors are important in stimulating synaptic activity that can lead to increased dendritic arbor growth (Cline, 2001). NMDA receptor antagonists significantly reduced dendritic branch dynamics, indicating dendritic arbor growth is dependent at some stage on NMDA receptor activity. For example, mice that had a loss-of-function mutation in the NMDA receptor 1 gene showed reduced dendritic arbor branch

dynamics in layer IV cortical neurons (Iwasato et al., 2000). In contrast, when AMPA receptors were blocked there was no effect on the dendritic arbor growth rate in young neurons (Cline, 2001). Thus the role of most glutamate receptors appears to involve enhancing branch dynamics in the dendritic arbor, leading to increased dendritic arborization when these receptors are stimulated (Jontes, Buchanan, & Smith, 2000). This increased dendritic arborization is then maintained over time by synapse formation on the newly added branches (Cline, 2001).

While studies of increased NMDA and glutamate receptor activity provide examples of how excitatory stimuli can increase dendritic arbor growth, the role of inhibitory inputs in dendritic development remains less well explored. A recent study (Shen, 2009) examined the role of afferent inhibitory GABA inputs on dendritic arborization of *Xenopus* optic tectal cells *in vivo*. Expression of a mutant peptide, which disrupts the anchoring of the inhibitory $GABA_A$ receptor ($GABA_AR$) to the membrane, blocked $GABA_AR$-mediated transmission in about 36% of the transfected neurons. $GABA_AR$-mediated synaptic current was also significantly reduced in the remaining transfected neurons (Shen, 2009). When the dendritic branch dynamics were examined it was found that blocking inhibitory GABA activity decreased arbor density, as seen by marked decreases in branch tip numbers without decreases in total dendritic branch length. The average branch segment length also decreased at the 48 and 72 hour imaging points (Shen, 2009). It should be noted, though, that the age points used here only extended to 72 hours, and developmental changes in dendritic arborization were not examined after 3 days of growth.

Mechanisms of Dendritic Growth Retardation and Stabilization

As important as it is for a neuron to develop sufficiently large dendrites, dendrites that are too large can lead to problems, such as severe mental retardation (Kaufmann & Moser, 2000). Other problems that can result from enlarged dendritic fields include synaptic overlap, in which the receptive field of the neuron with the enlarged dendrite receives synaptic input that is targeted for other neurons, resulting in degradation of information transfer (Cline, 2001). Thus mechanisms that restrict and limit dendritic arbor growth play in important role in forming stable, mature neural connections.

One such mechanism involves the calcium/calmodulin-regulated serine/threonine kinase, CaMKII. This kinase is heavily expressed in dendrites, and its enzymatic activity is greatly increased in the presence of strong synaptic input (Soderling, 2000). In optic tectal neurons, slower dendritic arbor growth rate corresponded temporally to the first detectable levels of CaMKII proteins (Wu & Cline, 1998). Elevated CaMKII activity was associated with decreases in both new branch additions and branch retractions, thus leading to overall dynamic stability. When pharmacological antagonists were used to block endogenous CaMKII, dendritic arbors grew to abnormally large sizes (Wu & Cline, 1998). Further support for a role of CaMKII in dendritic stabilization comes from a study in which viral vector-mediated over-expression of CaMKII in optic tectal neurons led to increased synaptic strength and termination of dendritic elaboration (Wu, Malinow, Cline, 1996). Thus, synaptic activity may be responsible for CaMKII-mediated increases in synaptic strength and retardation of dendritic arbor growth at a certain point in the mature neuron.

Synaptic activity has also been shown in the *Xenopus* retinotectal system, as well as in vertebrate retinal ganglion cells, to refine dendritic branch additions by recruiting

specific neurotransmitter receptors to sites of synaptic contact (Cline, 2001; Wong & Ghosh, 2002). Initially, newly extended axonal branches only synapse at sites with postsynaptic NMDA receptors, but as synapses mature AMPA receptors are recruited to the synaptic sites (Cline, 2001). The presence of AMPA receptors in the synapse helps to stabilize the branches on which the synapses are located and, once these branches are stabilized, new branches may be added. These secondary branches in turn establish more synapses with only NMDA receptors, which may eventually stabilize or retract depending on whether AMPA receptors are recruited, and the cycle continues. When synapses form and no AMPA receptors are recruited, the axonal branches on those synapses retract (Cline, 2001).

Present Study

We have shown above that stimulus-elicited activity in the CT and lingual-tonsilar IXth nerves are likely to alter substantially during the first few weeks of postnatal life in hamster (Hill, 1988; Harada & Maeda, 2004). Specifically, taste receptor cells that provide the physiological basis for stimulus-generated afferent activity proliferate and become functional between about 7 and 21 days of age (Miller and Smith, 1988; Belecky and Smith, 1990), while at least three age-dependent shifts in CT nerve stimulus sensitivity occur between about 10 and 100 days of age (Hill, 1988; R. Stewart, unpublished observation). Other work shows that dendritic arborization is enhanced by increased synaptic activity, and later stabilized by stimulus-elicited, patterned activity (Luo et al., 1996; Cline, 2001; Wong & Ghosh, 2002). Based on these combined findings we predict that the dendritic arbors of the neurons within the NTS of normally-reared hamsters will experience high rates of growth during the first few weeks of postnatal development, and then show a

period of dendritic retraction prior to acquisition of mature, unchanging dendritic morphology. Recent research has shown that dendritic arbor elaboration is a rather common process during development (Cline, 2001; Wong & Ghosh, 2002; Shen et al., 2009), while dendritic arbor retraction is less commonly observed, although still part of normal development (Liu, Schweitzer, Renehan, 2000; Luo & O'Leary, 2005).

Dendritic arbor development of salt-responsive neurons in the rat NTS has been shown to undergo rapid growth during early postnatal development, followed by retraction and stabilization of arbors (Liu, Schweitzer, Renehan, 2000). Liu et al. (2000) hypothesized that the biphasic change in dendritic morphology they reported was due to the increase in gustatory Na^+ sensitivity observed in rat between about 10 and 45 days of age. We anticipate that the dendritic architecture of neurons in the neonatal hamster NTS will undergo morphological changes reminiscent of those reported in rat. The effects of afferent synaptic activity on dendritic arbor development of NTS neurons have not been examined in hamsters, however. Therefore this study will explore whether dendritic arbors of hamster NTS neurons do indeed undergo elaboration during early periods of increased patterned synaptic activity followed by retraction and stabilization as the peripheral taste system approaches functional maturity at around 90 days of age (Hill, 1988). In addition, we will test the idea that afferent activity drives dendritic development in the postnatal hamster NTS by performing unilateral cuts of LT-IX. Specifically, we predict that nerve cuts performed at about the time of weaning will permit early elaboration of dendritic arbors but preclude or severally diminish pruning and stabilization. This effect could be manifested as either abnormally large dendritic arbors (lack of pruning) or abnormally small dendritic arbors (arbor collapse due to lack of stabilization) in the NTS of

adult hamster that were subjected to unilateral section of LT-IX around weaning. The taste system provides a unique advantage in studies such as the one proposed here, because NTS is virtually ipsilateral and thus can serve as an internal, within subject control.

METHODS

Animals and Golgi-Cox Staining

All animals used in this experiment were Syrian Golden hamsters, reared and manipulated in accordance with protocols approved by the Washington and Lee University Institutional Animal Care and Use Committee. The lingual tonsilar branch of the glossopharyngeal nerve (IX^{th} cranial nerve) was cut unilaterally on the right side at 18 days of age under Nembutal anesthesia (90 mg/kg, IP) according to methods published elsewhere (Reidy et al., 2008). Animals were subjected to either nerve cut or sham nerve cut (in which the nerves were exposed surgically but left unmanipulated) and sacrificed at 31 (3 animals), 65 (4 animals), and 96 (2 animals) days post-surgery. These groups are hereafter referred to by their ages at time of sacrifice – namely 49, 83, and 114 days of age, respectively – since this is helpful for understanding the normative dendritic development observed on the uncut-side of the NTS. Separate groups of hamsters were allowed to develop without any surgical manipulation and sacrificed at various age points up to 67 days postnatal to examine normative dendritic development.

A modified Golgi-Cox staining technique was used to visualize the neurons. The technique, first described by Glasser and van der Loos (1981), was modified to allow for better vibratome sectioning post-staining (Gibb & Kolb, 1998). The brains were excised immediately after the animals were sacrificed by overdose with urethane (2.4 mg/kg, IP), and the hindbrain, cerebellum, and cortex were blocked and placed in the Golgi-Cox

solution (1% $K_2Cr_2O_7$, 1% $HgCl_2$, 0.8% K_2CrO_4 in dH_20). Specimens were left in Golgi-Cox solution in the dark for 24 days for the unmanipulated animals and 28 days for the animals that received unilateral glossopharyngeal transection. After this impregnation period the brains were removed and placed in 30% sucrose solution for 14 days.

Horizontal 150μm sections of hindbrain were cut using a vibratome (Leica VT-1000S, Leica Microsystems, Bannockburn, IL) . These sections were mounted on SuperFrost Plus slides (Fisher Scientific, Fair Lawn, New Jersey) and stained following the Gibb and Kolb (1998) protocol, substituting 2.5% sodium thiosulfate for Kodak Fix. Slides were dehydrated through graded alcohols, cleared in xylenes and coverslipped using Permount.

Imaging and Tracing

Neurons were imaged using a Leica upright transmitted light microscope and traced in real-time at 40X using Neurolucida image analysis and motorized stage control software (MBF Biosciences, Williston, VT). Dendrites were traced through 3 dimensional space and the total branch length, segment branch length, number and type of nodes, as well as cell body cross-sectional area were measured and recorded. During the tracing neurons were classified as either Class I or Class II, according to the classification scheme devised by Davis and Jang (1988). Class I neurons are fusiform and are characterized by long, relatively unbranched dendrites which may extend beyond the cytoarchitectonic boundaries of the gustatory region of the NTS. Class II neurons are multipolar and posses more dendrites of higher complexity than Class I, though their dendrites tend not to extend as far from the cell soma as Class I. Both classes tend to have spine poor dendrites and are oriented in the horizontal plane. Neurons were classified after the tracing as either Class I

or Class II based primarily on a quick broad overview of dendritic morphology – if the dendrites were elaborate and projected from all points along the perimeter of the cell body, a Class II distinction was assigned, while a Class I assignment was reserved for dendrites that branched less often and projected from only two points on the perimeter of the cell body.

Total dendrite length, total number of dendritic nodes, and cell body size were used as parameters of dendritic development (Jacobs et al., 2001) and measured in the traced neurons. In addition the primary, secondary, and tertiary dendritic branch lengths were quantified and measured. Dendrite and cell body measurement data were analyzed with multivariate analyses of variance, followed by Tukey HSD post-tests where appropriate, except for comparisons between cut- and uncut sides within age-groups. These *a priori* comparisons were made using two-tailed, independent Student t-tests. Alpha level was set at 0.05 for both Tukey HSD and t-tests.

RESULTS

Representative Neurons and Tracings

The brains of animals that were examined for normative developmental patterns of dendrite growth remained in the Golgi-Cox solution for 24 days, which resulted in NTS neurons that were inadequately impregnated to allow morphometric analyses. As a result, only brains from those animals that were surgically manipulated and remained in Golgi-Cox for 28 days were examined for dendritic morphology. This four day difference in impregnation time may be only partly responsible for the drastically different levels of impregnation. Another factor may be the age of the Golgi-Cox solution, which was about 60 days older when used to stain the brains of surgically-manipulated animals. Others have

observed superior impregnation with older Golgi-Cox solutions (P.C. Brunjes, personal communication). The IXth nerve projects ipsilaterally to the NTS, and hence neurons in the right NTS received reduced synaptic input while neurons in the left NTS received normal levels of synaptic input. The present results therefore represent dendrites obtained from nerve-cut animals only.

Representative neurons are shown from a 49 day old animal in Figure 4, which highlights the boundaries of the NTS and the distinguishing features of Class I and Class II neurons. The highlighted region in Figure 4a depicts the NTS in full, extending upwards on both sides from the midline in a heart-shaped pattern. The IXth nerve projects mainly to the rostral NTS (Stewart et al., 2005; May & Hill, 2006), which is highlighted at higher magnification in Figure 4b. Only neurons located in the rostral third of the NTS were traced. Within the rostral NTS the two classes of neurons are clearly distinguishable. Class I neurons (Figure 4c) are fusiform in shape and have dendritic projections which branch less often and later. Class I neurons also often have dendritic projections that extend beyond the cytoarchitectural boundaries of the NTS. Class II neurons (Figure 4d) are more multipolar in shape and have dendritic processes that branch sooner and with greater frequency than Class I neurons. Class II neurons also have dendritic trees that are more compact than Class I neurons. Because of it is difficult to image a single neuron and all of its dendrites as they extend in the image z-plane, Figures 4c and 4d depict the cell body and the bases of the proximal dendritic processes as they extend from the cell body. This is to emphasize the fusiform versus multipolar morphologies of Class I and Class II neurons, respectively.

Representative tracings of Class I and Class II neurons are shown in Figure 5. The tracings were made using Neurolucida and each different color branch reflects a uniquely different dendrite on that particular neuron. Class I neurons (5a and 5b) posses a more bipolar shape with fewer dendrites that exhibit less complex branching patterns compared to Class II neurons (5c and 5d). In contrast, Class II neurons are multipolar with more highly complex branching patterns than Class I neurons, and have dendritic branches which frequently overlap. All representative tracings are taken from a 49 day-old animal and shown at arbitrary magnifications, since Neurolucida fits each tracing to fill the display window. All length measurements are kept intact by the program, however, and were used for quantitative morphometric analysis using the NeuroExplorer module in Neurolucida. In each post-nerve cut survival group, cut-side NTS neurons from all animals were pooled, as were NTS neurons from the uncut-side. Then, neurons from cut- or uncut-side were further segregated morphologically into Class I and Class II sub-groupings.

Results for Total Dendritic Length, Total Number of Dendritic Branch Nodes, and Cell Body Area

Once all neurons were classified as Class I or Class II, and the quantitative measures of dendrite morphology and cell structure recorded, an analysis of total dendritic length, total number of dendritic nodes, and cell body area was performed. Means and standard errors for these variable are provided in Table 1. A multivariate analysis of variance (MANOVA) by neuron class was performed where the independent variables were age at sacrifice and NTS side (i.e., cut or uncut) and the dependent variables were total dendritic length, cell body area, and total branch node number. 51 Class I neurons and 52 Class II neurons were examined.

For Class I neurons there were significant main effects of age at sacrifice for total dendritic length [$F(2, 50) = 26.696$, $p < 0.001$], total number of branch nodes [$F(2,50) = 15.375$, $p < 0.001$], and cell body cross-sectional area [$F(2, 50) = 9.839$, $p < 0.001$]. Among these neurons there were also significant main effects of cut condition for total dendritic length [$F(1, 50) = 11.789$, $p < 0.001$], and total number of branch nodes [$F(1, 50) = 10.214$, $p < 0.01$], but not for cell body cross-sectional area [$F(1, 50) = 0.652$]. In addition to these main effects there were also significant interaction effects between age at sacrifice and cut condition for total dendritic length [$F(2, 50) = 12.219$, $p < 0.001$] and total number of branch nodes [$F(2, 50) = 7.678$, $p < 0.001$], but not cell body cross-sectional area [$F(2,50) = 1.720$].

For Class II neurons there were significant main effects of age at sacrifice for total dendritic length [$F(2, 51) = 11.692$, $p < 0.001$) and total number of branch nodes [$F(2, 51) = 15.628$, $p < 0.001$], but not cell body cross-sectional area [$F(2, 51) = 1.474$]. Among these neurons there were also significant main effects of cut conditions for total dendritic length [$F(1, 51) = 15.222$, $p < 0.001$] and total number of branch nodes [$F(1, 51) = 6.964$, $p < 0.05$], but not for cell body cross-sectional area [$F(1, 51) = 3.116$). Additionally there was a significant interaction between age at sacrifice and cut condition for total dendritic length [$F(2, 51) = 4.042$, $p < 0.05$]. A series of post-hoc Tukey HSD tests and t-tests were performed to investigate these differences further.

Investigating total dendritic branch length across the various ages indicated that the youngest animals had significantly longer cut-side NTS neuron dendrites than did older animals. These results are summarized in in Figure 6. Class I neurons had average total dendritic branch lengths of cut-side neurons from 49 day-old animals (M = 1340.5μm, SE =

105.9μm) that were significantly greater than those of cut-side neurons in either the 83 day-old (*M* = 443.3μm, *SE* = 69.0μm) or the 114 (*M* = 533.5μm, *SE* = 96.8μm) day-old animals. Class II neurons similarly had total dendritic branch lengths of cut-side neurons in 49 day-old animals (*M* = 2293.0μm, *SE* = 181.0μm) that were significantly greater than those of cut-side neurons in either the 83 day-old (*M* = 1178.6μm, *SE* = 173.9μm) or 114 day-old animals (*M* = 1152.5μm, *SE* = 259.8μm).

Interestingly, the effect of unilateral nerve cut on total dendritic branch length was restricted to the shortest post-cut survival time. In 49 day-old animals, total dendritic branch lengths of cut-side Class I neurons (*M* = 1340.5μm, *SE* = 105.9μm) were significantly greater than those of uncut-side neurons (*M* = 627.4μm, *SE* = 87.7μm). The same effect was seen in Class II neurons, with neurons in the cut condition (*M* = 2293.0μm, *SE* = 181.0μm) being significantly longer than neurons in the uncut condition (*M* = 1141.4μm, *SE* = 100.1μm), but only in the 49 day-old animals. No significant differences between uncut- versus cut-side neuron dendritic branch lengths were observed in the 83 or 114 day-old age groups.

The total number of nodes (branch points) along the dendritic processes of each neuron were tallied, pooled according to class, and compared among post-nerve cut survival times. These results are presented in Figure 7. Cut-side Class I neurons of 49 day-old animals had significantly more nodes (*M* = 10.2, *SE* = 1.6) compared to cut-side Class I neurons in either 83 day-old (*M* = 3.1, *SE* = 0.8) or 114 day-old animals (*M* = 3.4, *SE* = 0.9) (Figure, 7a). This pattern was also observed for Class II cut-side neurons (Figure 7b), with 49 day-old animals having significantly more nodes (*M* = 18.0, *SE* = 1.2) than cut-side neurons in either 83 day-old (*M* = 8.0, *SE* = 1.3) or 114 day-old animals (*M* = 7.2, *SE* = 1.3).

Within each age group, the only significant difference in total number of nodes between cut- and uncut-side neurons occurred for the 49 day-old animals. Among Class I neurons, those located on the cut-side of the 49 day-old animals (M = 10.2, SE = 1.6) contained significantly more nodes than neurons in the uncut-side (M = 4.1, SE = 0.7). For the Class II neurons in 49 day-old animals, cut condition neurons (M = 18.0, SE = 1.2) having significantly more nodes than uncut condition neurons (M = 10.4, SE = 1.5). Finally, Class II neurons consistently displayed more nodes than Class I neurons, as expected (Davis and Jang, 1988).

Mean cell body areas are presented in Figure 8. While the effect of nerve-cut on cell body cross-sectional area is significant, it appears to be less pronounced than effects on dendrite morphology. Specifically, cut-side Class I neurons (Figure 8a) in 49 day-old animals (M = 364.7μm^2, SE = 54.9μm^2) have significantly larger cell body cross-sectional areas than those observed in 83 day-old (M = 205.4μm^2, SE = 33.6μm^2) or 114 day-old animals (M = 197.6μm^2, SE = 33.6μm^2). The same pattern was seen for cut-side Class II neurons (Figure 8b), with 49 day-old animals (M = 454.2μm^2, SE = 59.4μm^2) possessing significantly larger cell body cross-sectional areas than those observed in 83 day-old (M = 370.4μm^2, SE = 58.7μm^2) and 114 day-old animals (M = 327.5μm^2, SE = 60.3μm^2). There was no significant difference in cell body cross-sectional area between cut and uncut conditions in any of the age groups. There also appeared to be greater variation in cell body cross-sectional areas in general. This may be attributable to variation in the cross-sectional plane at which was cell body measurements were taken.

Primary, Secondary, and Tertiary Dendritic Segment Lengths

In an effort to identify the origin of nerve-cut-induced differences in dendritic branch morphology, primary, secondary, and tertiary dendritic segment lengths were investigated. The total length of each segment type was summated per neuron, and then summated values were used for comparisons among post-cut survival times. Since Class I and Class II neurons are characterized by different segment lengths depending on the degree of branching, they were once again separated during the analysis. Branch order length results are presented graphically in Figure 9, and the summary data are presented in Table 2.

MANOVA revealed that among Class I neurons tertiary dendritic segment length was significantly different among ages [$F(2, 50) = 4.404$, $p < 0.05$] and between cut condition [$F(1,50) = 4.657$, $p < 0.05$] (Figure 9e). There was also a significant interaction effect between cut condition and age at sacrifice [$F(2,50) = 3.821$, $p < 0.05$] for tertiary dendritic segment length in Class I neurons. A MANOVA for Class II neurons also revealed a significant main effect of age at sacrifice on tertiary dendritic segment length [$F(2, 51) = 4.772$, $p < 0.05$] and a main effect of cut condition on tertiary dendritic segment length [$F(1,51) = 5.991$, $p < 0.05$] (Figure 9f). There was also a significant main effect of age at sacrifice on primary dendritic segment length [$F(2,51) = 3.211$, $p < 0.05$] (Figure 9b). Once again a series of post-hoc Tukey-HSD tests and t-tests were done to examine these differences in greater depth.

Investigating dendritic segment lengths across age reveals some interesting differences. Among Class I neurons, secondary order segments were significantly longer in the 49 day-old animals – both among the cut condition ($M = 365.37$μm, $SE = 83.75$) and uncut condition ($M = 299.32$μm, $SE = 69.66$μm) – than secondary order segments in 83

day-old animals within the cut condition (*M* = 187.88μm, *SE* = 27.44μm) and uncut condition (*M* = 180.32μm, *SE* = 32.50μm) (Figure 9c). Tertiary segments were significantly longer in the cut condition Class I neurons in the 49 day-old animals (*M* = 405.45μm, *SE* = 75.25μm) than in the 83 day-old animals (*M* = 117.88μm, *SE* = 29.45μm) (Figure 9e).

Among Class II neurons primary segment lengths of cut condition neurons in the 114 day-old animals (*M* = 305.43μm, *SE* = 67.06μm) were significantly longer than neurons in either the cut or uncut conditions in the two earlier age groups (Figure 9b). This was a strange finding between the age groups not seen in any of the other results, and may hold unique for primary segment length in Class II neurons. Tertiary segment lengths for cut condition Class II neurons in the 49 day-old animals (*M* = 607.41μm, *SE* = 70.37μm) were significantly longer than any of the other groups (Figure 9f). Interestingly Class II neurons in the uncut condition in 114 day old animals (*M* = 123.46μm, *SE* = 26.19μm) were significantly shorter than uncut condition neurons in any other age group (Figure 9f).

Sham-operated Control Animals

Two animals were sham operated at 18 days postnatal. Only one of these animals survived, and it was sacrificed at 49 days. Total dendritic length, the total number of nodes, and cell body size were examined among 19 neurons in the NTS, and Data is shown in Table 3. Results are presented in Figure 10. There were no significant differences between the left and right NTS among any of the measured variables. In general, values for these variables resembled those obtained for uncut-side neurons in the 49 day-old nerve-cut group.

DISCUSSION

The results of the present study demonstrate that unilateral glossopharyngeal section at 18 days of age results in significant changes in ipsilateral gustatory NTS neuron morphology following a 31 day post-nerve cut survival time. More specifically, total length of dendrites, total number of dendritic branch points, and soma areas of Class I and Class II rostral NTS neurons ipsilateral to the nerve cut are significantly increased compared to those contralateral to nerve cut. Remarkably, nerve cut-dependent alterations in dendritic and soma morphometry are absent in the brains of animals allowed a 65 day post-nerve cut survival time.

Taken together, these results indicate that dendritic pruning dependent on synaptic input may occur in the developing hamster taste system, though the exact time point of this pruning activity remains unclear. One interpretation of the present results is that cutting the lingual-tonsilar branch of the glossopharyngeal (IXth) nerve arrests dendritic development in a more elaborate state, although very interestingly the dendrites can still undergo pruning if allowed to develop long enough. Studies have shown that this specific branch of the IXth nerve selectively projects to the rostral NTS (Stewart et al., 2005; May and Hill, 2006), and hence the nerve cuts performed in this study certainly remove some of the afferent synaptic activity to this area. Anatomical data from hamster suggest that at the time of nerve cut in the present study (18 days postnatal), taste buds of the circumvallate papilla are few in number and immature morphologically (Miller and Smith, 1988). Thus, nerve cut may preclude influences of taste stimulus-elicited activity in shaping dendritic arbors of NTS neurons that receive synaptic input from glossopharyngeal nerve.

The exclusive effects of nerve cuts on ipsilateral NTS neurons make it tempting to speculate that the changes in dendritic morphology observed in the results are directly

linked to the loss of normal afferent synaptic activity. The results from the sham surgery animal solidify the argument that changes in afferent activity are involved in altered dendritic morphology, since NTS neurons in this animal resembled those on the uncut-side NTS in age-matched experimental animals. However, the present data leave open two alternative explanations for the exuberant dendritic morphology induced by nerve cut. One possibility is that loss of glossopharyngeal axonal inputs induces local changes that promote elongation and branching of dendrites. Another possibility is that the nerve cut interrupts or delays normal dendritic pruning. One straightforward way to distinguish between these two possibilities is to examine normal postnatal development of dendritic arbor morphology.

The youngest animals examined were sacrificed 31 days after the nerve cuts, at 49 days-old. Unfortunately none of the unmanipulated control animals sacrificed at 18 days of age – the age at which the nerve cuts were made – had brains adequately stained to allow morphometric characterization of their dendritic fields. If a nerve cut limits, delays, or interrupts normal dendritic pruning, then we would predict the dendritic morphologies of Class I and Class II NTS neurons in 18 day-old hamsters to resemble those of Class I and Class II cut-side NTS neurons in 31 day post-nerve cut hamsters. Alternatively, if nerve cut induces elongation and branching of dendrites, one would expect rostral NTS neurons in 18 day-old hamsters to exhibit more compact, less branched dendritic arbors.

The dendritic morphology of NTS neurons ipsilateral to glossopharyngeal section in 49 day-old animals was vastly different than the morphology of all other neurons examined. They had far longer processes, more complex branching patterns as indicated by increased nodes, and larger cell bodies. The differences between dendritic parameters of

cut- and uncut-side neurons in 49 day-old animals - especially total dendritic length – was dramatic. Yet by the next post-nerve cut survival point – 83 days-old – the dendrites exhibited features that resembled those seen in the NTS contralateral to nerve cut at 31 days survival. At 83 days of age, there was no longer any difference between the cut and uncut sides of the NTS. This apparent recovery of normal dendritic morphology appeared to be permanent: no differences of any kind in dendritic morphology were detected between the 83 day-old and 114 day-old animals. Perhaps this abnormally late-stage pruning is due to rearrangement of the major gustatory nerve terminal fields. It has been shown previously that gustatory primary afferent projections are capable of rearrangement when their ability to "interpret" stimuli is compromised (Mangold and Hill, 2007; Mangold and Hill, 2008). In the present study, it may be that when the IXth nerve is cut, the terminal fields of the CT and GSP nerves sprout and invade territory previously occupied by IXth nerve to compensate for the lack of IXth nerve input.

Our results indicate that such rearrangement must require more than 31 days to occur, and by about 60 days after the cut there would be nearly complete terminal field rearrangement. This would restore nominal synaptic activity and contribute to pruning of the exuberant dendritic arbors. A method to confirm this would be to label the terminal fields of the three taste nerves in a manner similar to that May and Hill (2006) used and then monitor the distribution of the terminal fields within the NTS between the time of the IXth nerve cut and 60 days afterwards. Based on previous work from our laboratory (Bradenham et al., 2006), expansion of GSP and CT fields dorsally and caudally within the rostral NTS would be predicted to occur.

Efforts to more conclusively localize the difference in dendritic lengths by examining specific segment types pointed towards the more distal segments. Tertiary dendritic segments were significantly longer on neurons in the cut-side of the NTS compared to uncut-side NTS of 49 day-old animals. Due to the inconsistency of neurons possessing quaternary and further dendritic branch segments, tertiary segments were the highest order branch analyzed, though the trend may have continued to include longer segments of higher order in the cut-side NTS of 49 day-old animals. Nonetheless it appears that the differences in total dendritic branch length may be due primarily to differences in higher order segment length, and possibly even the frequency of higher order segments.

Possible Mechanisms for Dendritic Pruning in the Gustatory System

There are many hypothesized mechanisms by which dendrites may undergo pruning. Afferent signals have been shown to be paramount for determining dendritic pruning. Afferent input modulation in Ca^{2+} signaling (Wong & Ghosh, 2002), NMDA signaling (Li, Aelst, and Cline, 2000) or $GABA_AR$-dependent transmission (Shen et al., 2009) are notable mechanisms that have been implicated in dendrite stabilization. Neurotransmission-related Ca^{2+} signals have been shown to sculpt dendritic arbors by encouraging foraging dendrites to remain in place once they receive afferent synaptic inputs (Wong & Ghosh, 2002). Since the dendrites in this study were more elaborate on the cut -side NTS, it is unlikely that they are sculpted exclusively by a Ca^{2+} dependent mechanism, since this would imply less branched neurons on the nerve cut side. Glutamate-dependent activity has been shown to regulate the Rho GTPases (Li, Aizenman, Cline, 2002), which are highly involved in regulating limiting branch additions and retractions (Li, Aelst, Cline, 2000). Our results seem to indicate that Rho GTPases are more

likely candidates for the dendritic pruning that occurs during gustatory development, since the dendritic pruning that occurs in cut-side NTS between 49 and 83 days of age may be due to synaptic rearrangement: synaptic connection and activity appears to reduce dendritic complexity rather than enhance it.

Further studies could examine the role of Rho GTPases by selectively labeling cells with active Rho GTPase molecules in the rostral NTS of animals that have undergone a IXth nerve cut compared to animals that have not. This could be done by labeling guanine nucleotide exchange factors (GEFs), which are proteins responsible for transforming the Rho protein to the active form and are a representation of Rho GTPase activity (Li, Aizenman, Cline, 2002). Since the baseline levels of Rho GTPases present should be equal in cut and uncut sides of NTS before nerve cut, and differences in dendritic morphology are predicted to be due to selective activation of the Rho GTPases, then increases in cut-side GEF labeling following nerve cut would correspond to increased active Rho GTPase.

Another way to examine the role of Rho GTPases in a hamster model would be selective activation of the rostral NTS neurons with glutamate, a known enhancer of Rho GTPase activity (Li, Aizenman, Cline, 2002). Animals could be exposed to nerve cuts, and then attempts to rescue the dendritic sculpting could be made by selectively applying glutamate to the terminal field areas of the cut nerves. All of these experiments are hypothetical, though, and before they are conducted normative dendritic development should be examined using Golgi-Cox staining at younger age points than those examined here.

Conclusions

It appears that afferent synaptic activity is involved in sculpting dendritic arbors of the developing central gustatory system, probably by reducing dendritic arbor complexity and expanse. Thirty-one days following IXth nerve cut at 18 days to reduce afferent activity, dendritic arbors of Class I and Class II neurons of the rostral NTS exhibited significantly increased size and complexity. Remarkably, these abnormally elaborate arbors appeared normal 83 days after nerve cut. Rearrangement of the terminal fields of the remaining CT and GSP taste nerves may be responsible for the delayed pruning seen in the aftermath of nerve injury during the suckling period. It appears that this reduction in dendritic branch size and complexity is due to pruning in the most distal segments of the dendrites, and may involve Rho GTPases as a mechanistic basis. It will be important to explore potential mechanistic bases for these changes, as well as the temporal limits on the dramatic morphological changes that attend iatrogenic insult to primary afferent axons and alteration of normal primary afferent function. Beyond the fundamental neurobiological implications of answers to these issues, the downstream consequences of early postnatal nerve injury on the development of taste-guided behaviors represents a particularly important avenue for investigation given the current global obesity crisis.

References

Alder E et al. (2000) A novel family of mammalian taste receptors. Cell 100: 693-702.

Altman J, Bayer SA (1980) Development of the brainstem in the rat. II. A thymidine radiographic study of the time of origin of neurons in the lower medulla. The Journal of Comparative Neurology 194: 1-35.

Bagri, A, Chen, HJ, Yaron, A, Pleasure SJ, Tessier-Lavigne, M (2003) Stereotyped pruning of long hippocampal branches triggered by retraction inducers of the semaphoring family. Cell 113: 285-299.

Belecky TL, Smith DV (1990) Postnatal development of palatal and laryngeal taste buds in the hamster. The Journal of Comparative Neurology 293: 646-654.

Bradley RM, Mistretta CM (1973) The gustatory sense in foetal sheep during the last third of gestation. The Journal of Physiology 231: 271-282.

Bradley RM, Mistretta CM (1980) Developmental changes in neurophysiological taste responses from the medulla in sheep. Brain Research 191: 21-34.

Bradenham BP, Harrison CH, Stewart JS, Stewart RE (2006) Chorda Tympani (CT), Greater Superficial Petrosal (GSP), and IXth nerve terminal fields in hamster Solitary Nucleus (NTS). Chemical Senses 31:

Chandrashekar J, Hoon MA, Ryba NJ, Zuker CS (2006) The receptors and cells for mammalian taste. Nature 444: 288-294.

Cline HT (2001) Dendritic arbor development and synaptogenesis. Current Opinion in Neurobiology 11: 118-126.

Davis BJ, Jang T (1988) A Golgi analysis of the Gustatory Zone of the Nucleus of the Solitary Tract in the adult hamster. The Journal of Comparative Neurology 278: 388-396.

Davis JD, Smith GP, Singh B, McCann DP (2000) The impact of mil-derived unconditioned and conditioned negative feedback on the microstructure of ingestive behavior. Physiology & Behavior 70: 279-285.

DeSimone JA, Lyall V (2006) Taste receptors in the gastrointestinal tract III. Salty and sour taste: Sensing of sodium and protons by the tongue. American Journal of Physiology – Gastrointestinal and Live Physiology 291: G1005-G1010.

Feller MB (1999) Spontaneous correlated activity in developing neural circuits. Neuron 22: 653-656.

Fulwiler CE, Saper CB (1984) Subnuclear organization of the efferent connections of the parabrachial nucleus in the rat. Brain Research Review 7: 229-259.

Gibb R, Kolb B (1998) A method for vibratome sectioning of Golgi-Cox stained whole rate brain. Journal of Neuroscience Methods 79: 1-4.

Glasser EM, van der Loos H (1981) Analysis of thick brain sections by obverse-reverse computer microscopy: applications of a new, high clarity Golgi-Nissl stain. Journal of Neuroscience Methods 4: 117-125.

Halsell CB (1998) Differential distribution of amygdaloid input across rostral solitary nucleus subdivisions in rat. Annals of the New York Academy of Sciences 855: 482-485.

Harada S, Smith DV (1992) Gustatory sensitivities of the hamster's soft palate. Chemical Senses 17: 37-51.

Harada S, Yamaguchi K, Kanemaru N, Kasahara Y (2000) Maturation of taste buds on the soft palate of the postnatal rat. Physiology & Behavior 68: 333-339.

Harada S, Maeda S (2004) Developmental changes in sugar responses of the chorda tympani nerve in preweanling rats. Chemical Senses 29: 209-215.

Heck GL, Mierson S, DeSimone JA (1984) Salt taste transduction occurs through an amiloride-sensitive sodium transport pathway. Science 223: 403-405.

Hill DL, Amli CR (1980) Ontogeny of chorda tympani nerve responses to gustatory stimuli in the rat. Brain Research 197: 27-38.

Hill DL, Mistretta CM, Bradley RM (1982) Developmental changes in taste response characteristics of rat single chorda tympani fibers. The Journal of Neuroscience 2: 782-790.

Hill DL, Bradley RM, Mistretta CM (1983) Development of taste responses in rat nucleus of solitary tract. The Journal of Neurophysiology 50: 879-895.

Hill DL, Bour TC (1985) Addition of functional amiloride-sensitive components to the receptor membrane: A possible mechanism for altered taste responses during development. Developmental Brain Research 20: 310-313.

Hill DL (1987) Development of taste responses in the rat parabrachial nucleus. Journal of Neurophysiology 57: 481-495.

Hill DL (1988) Development of chorda tympani nerve responses in the hamster. The Journal of Comparative Neurology 268: 346-356.

Hill DL, May OL (2007) Development and plasticity of the gustatory portion of nucleus of the solitary tract. In: The role of the nucleus of the solitary tract in gustatory processing (Bradley RM ed.), pp17-38. New York: CRC Press.

Huang AL et al. (2006) The cells and logic for mammalian sour taste detection. Nature 442: 934-938.

Iwasato T, Datwani A, Wolf AM, Nishiyama H, Taguchi Y, Tonegawa S, Knopfel T, Erzurumlu RS, Itohara S (2000) Cortex-restricted disruption of NMDAR1 impairs neuronal patterns in the barrel cortex. Nature 406: 726-731.

Jacobs B, Schall M, Prather M, Kapler E, Driscoll L, Baca S, Jacobs J, Ford K, Wainwright M, Tremi M (2001) Regional dendritic and spine variation in human cerebral cortex: a quantitative Golgi study. Cerebral Cortex 11, 558-571.

Jontes JD, Buchanan J, Smith SJ (2000) Growth cone and dendrite dynamics in zebrafish embryos: Early events in synaptogenesis imaged *in vivo*. Nature Neuroscience 3: 231-237.

Karimnamazi H, Travers JB (1998) Differential projections from gustatory responsive regions of the parabrachial nucleus to the medulla and forebrain. Brain Research 813: 283-302.

Katz LC, Shatz CJ (1996) Synaptic activity and the construction of cortical circuits. Science 274: 1132-1138.

Kaufmann WE, Moser HW (2000). Dendritic abomalies in disorders associated with mental retardation. Cerebral Cortex 10: 981-991.

King CT, Hill DL (1993) Neuroanatomical alterations in the rat nucleus of the solitary tract following early maternal NaCl deprivation and subsequent NaCl repletion. The Journal of Comparative Neurology 333: 531-542.

King MS (2007) Anatomy of the rostral nucleus of the solitary tract. In: The role of the nucleus of the solitary tract in gustatory processing (Bradley RM ed.), pp17-38. New York: CRC Press.

Kondoh T, Toril K (2008) MSG intake suppresses weight gain, fat deposition, and plasma leptin levels in male Sprague-Dawley rats. Physiology & Behavior 95: 135-144.

Kunishima N et al. (2000) Structural basis of glutamate recognition by a dimeric metabotropic gltamate receptor. Nature 407: 971-977.

Lasiter PS, Kachele DL (1988) Postnatal development of the parabrachial gustatory zone in rat: dendritic morphology and mitochondrial enzyme activity. Brain Research Bulletin 21: 79-94.

Lasiter PS, Wong DM, Kachele DL (1989) Postnatal development of the rostral solitary nucleus in rat: dendritic morphology and mitochondrial enzyme activity. Brain Research Bulletin 22: 313-321.

Lasiter PS (1992) Postnatal development of gustatory recipient zones within the nucleus of the solitary tract. Brain Research Bulletin 28: 667-677.

Li Z, Aelst LV, Cline HT (2000) Rho GTPases regulate distinct aspects of dendritic growth in *Xenopus* central neurons *in vivo*. Nature Neuroscience 3: 217-225.

Li Z, Aizenman CD, Cline HT (2002) Regulation of Rho GTPases by crosstalk and neuronal activity *in vivo*. Neuron 33: 741-750.

Li CS, Cho YK, Smith DV (2002) Taste responses of neurons in the hamster solitary nucleus are modulated by the central nucleus of the amygdala. The Journal of Neurophysiology 88: 2979-2992.

Liu YS, Schweitzer L, Renehan WE (2000) Development of salt-responsive neurons in the nucleus of the solitary tract. The Journal of Comparative Neurology 425, 219-232.

Luo L et al. (1996) Differential effects of the Rac GTPase on Purkinje cell axons and dendritic trunks and spines. Nature 379: 837-840.

Luo L, O'Leary DDM (2005) Axon retraction and degeneration in development and disease. Annual Review of Neuroscience 28: 127-156.

Lyall V et al. (2004) The mammalian amiloride-insensitive non-specific salt taste receptor is a vanilloid receptor-1 variant. The Journal of Physiology 558: 147-159.

May OL, Erisir A, Hill DL (2005) A comparative analysis of the ultrastructural morphology of the three gustatory nerve axons in the nucleus of the solitary tract in developmentally sodium-restricted and control rats. Chemical Senses 30: A167.

May OL, Hill DL (2006) Gustatory terminal field organization and developmental plasticity in the nucleus of the solitary tract revealed through triple fluorescent labeling. The Journal of Comparative Neurology 497: 658-669.

Mangold JE, Hill DL (2007) Extensive reorganization of primary afferent projections into the gustatory brainstem induced by feeding a sodium-restricted diet during development: Less is more. The Journal of Neuroscience 27: 4650-4662.

Mangold JE, Hill DL (2008) Postnatal reorganization of primary afferent terminal fields in the rat gustatory brainstem is determined by prenatal dietary history. The Journal of Comparative Neurobiology 509: 594-607.

Miller, IJ, Smith, DV (1984) Quantitative taste bud distribution in the hamster. Physiology & Behavior 32: 275–285.

Miller, IJ, Smith, DV (1988) Proliferation of taste buds in the foliate and vallate papillae of postnatal hamsters. Growth, Development, and Aging 52: 123-131.

Milner LD, Landmesser LT (1999) Cholinergic and GABAergic inputs drive patterned spontaneous motorneuron activity before target contact. The Journal of Neuroscience 19: 3007-3022.

Mistretta CM (1972) Topographical and histological study of the developing rat tongue, palate, and taste buds. In: Third symposium on oral sensation and perception: the mouth of the infant (Bosma JF ed.), pp163-187. Springfield, IL: Charles C. Thomas.

Ninomiya Y, Tanimukai T, Yoshida S, Funakoshi M (1991) Gustatory neural responses in preweanling mice. Physiological Behavior 49: 913-918.

Norgren R (1974) Gustatory afferents to ventral forebrain. Brain Research 81: 285-295.

Norgren R (1976) Taste pathways to hypothalamus and amygdala. The Journal of Comparative Neurology 166: 17-30.

Norgren, R (1995) Gustatory system. In: The Rat Nervous System (Paxinos G ed.) Chap 29. New York: Academic Press.

Nelson G et al. (2001) Mammalian sweet taste receptors. Cell 106: 381-390.

Nelson, G. et al. (2002) An amino-acid taste receptor. Nature 416: 199-202.

O'Leary, DDM, Bicknese, AR, De Carlos, JA, Heffner, CD, Koester, SE, et al. (1990) Target selection by cortical axons: alternative mechanisms to establish axonal connections in the developing brain. Cold Spring Harbor Symposium on Quantitative Biology 55: 453–468.

O'Leary, DDM, Stanfield, BB (1989) Selective elimination of axons extended by developing cortical neurons is dependent on regional locale. Experiments utilizing fetal cortical transplants. The Journal of Neuroscience 9: 2230–2236.

Rajan I, Cline HT (1998) Glutamate receptor activity is required for normal development of tectal cell dendrites *in vivo*. Journal of Neuroscience 18: 7836-7846.

Reidy BL et al. (2008) Developmental alteration of hamster chorda tympani nerve terminal field morphology. Presented at the Annual Meeting of the Society for Neuroscience, Washington, D.C., 2008.

Roper SD (2009) Parallel processing in mammalian taste buds? Physiology & Behavior 97, 604-608.

Ruthazer ES, Aizenman CD (2010) Learning to see: Patterned visual activity and the development of visual function. Trends in Neuroscience 33: 183-192.

Scott TR, Mark GP (1987) The taste system encodes stimulus toxicity. Brain Research 414: 197-203.

Shatz CJ (1996) Emergence of order in visual system development. The Proceedings of the National Academy of Sciences USA 93: 602-608.

Shen W, Da Silva JS, He H, Cline HT (2009) $GABA_A$R-dependent synaptic transmission sculpts dendritic arbor structure in Xenopus tadpoles *in vivo*. Journal of Neuroscience 29: 5032-5043.

Smith DV, Li CS (2000) GABA-mediated corticofugal inhibition of taste-responsive neurons in the nucleus of the solitary tract. Brain Research 858: 408-415.

Smith DV, Davis BJ (2000) Neural representation of taste. In: The Neurobiology of Taste and Smell. (Finger TE, Silver WL, Restrepo D eds.) pp. 353-394. New York: Wiley-Liss.

Soderling TR (2000) CaM-kinases: modulators of synaptic plasticity. Current Opinions in Neurobiology 10: 375-380.

Sollars, SI, Hill, DL (2005) *In vivo* recordings from rat geniculate ganglia: Taste response properties of individual greater superficial petrosal and chorda tympani neurons. The

Journal of Physiology 564: 877-893.

Sollars SI, Walker BR, Thaw AK, Hill DL (2006) Age-related decrease of the chorda tympani nerve terminal field in the nucleus of the solitary tract is prevented by dietary sodium restriction during development. Neuroscience 137: 1229-1236.

Srivastava, HC, Vyas, DC (1979) Postnatal development of the rat soft palate. Journal of Anatomy 128: 97-105.

Stanfield, BB, O'Leary, DDM(1985) Fetal occipital cortical neurons transplanted to rostral cortex develop and maintain a pyramidal tract axon. Nature 313:135–37.

Stewart RE, Hill DL (1993) The developing gustatory system: Functional, morphological and behavioral perspectives. In: Mechanisms of taste transduction (Simon SA, Roper SD ed.), pp127-158. London: CRC Press.

Stewart RE, DeSimone JA, Hill DL (1997) New perspectives in gustatory physiology: Transduction, development, and plasticity. American Jounral of Physiology 272: C1-C25.

Stewart RE, Chastain M, Selby A, Stewart J (2005) Extensive anatomical overlap of greater superficial petrosal (GSP) and IXth nerve terminal fields in hamster solitary nucleus (NTS). Chemical Senses 30:

Streefland C, Jansen K (1999) Intramedullary projections of the rostral nucleus of the solitary tract in the rat: gustatory influences on autonomic output. Chemical Senses 24: 655-664.

Travers SP, Norgren R (1995) Organization of orosensory responses in the nucleus of the solitary tract of the rat. Journal of Neurophysiology 73: 2144-2162.

Weliky, M, Katz, LC (1997) Disruption of orientation tuning in visual cortex by artificially

correlated neuronal activity. Nature 386: 680-685.

Whitehead MC, Bergula A, Holliday K (2000) Forebrain projections to the rostral nucleus of the solitary tract in the hamster. The Journal of Comparative Neurology 422: 429-447.

Whitehead, MC, Kachele, DL (1994) Development of fungiform papillae, taste buds, and their innervation in the hamster. The Journal of Comparative Neurology 340: 515-530.

Wolf G (1968) Projections of thalamic and cortical gustatory areas in the rat. The Journal of Comparative Neurology 132: 519-529.

Wong, ROL, Ghosh, A (2002) Activity-dependent regulation of dendritic growth and patterning. Nature Reviews, Neuroscience 3: 803-812.

Wu GY, Malinow R, Cline HT (1996) Maturation of a central glutamatergic synapse. Science 274: 972-976.

Wu GY, Cline HT (1998) Stabilization of dendritic arbor structure *in vivo* by CaMKII. Science 279: 222-226.

Wu GY, Zou DJ, Rajan I, Cline HT (1999) Dendritic dynamics *in vivo* change during neuronal maturation. Journal of Neuroscience 19: 4472-4483.

Yamada T (1980) Chorda tympani responses to gustatory stimuli in developing rats. Japanese Journal of Physiology 30: 631-643.

Yuste R, Nelson DA, Rubin WW, Katz LC (1995) Neuronal domains in developing neocortex: mechanisms of coactivation. Neuron 14: 7-17.

Zhao et al. (2003) The receptors for mammalian sweet and umami taste. Cell 115: 255-266.

Figures and Tables

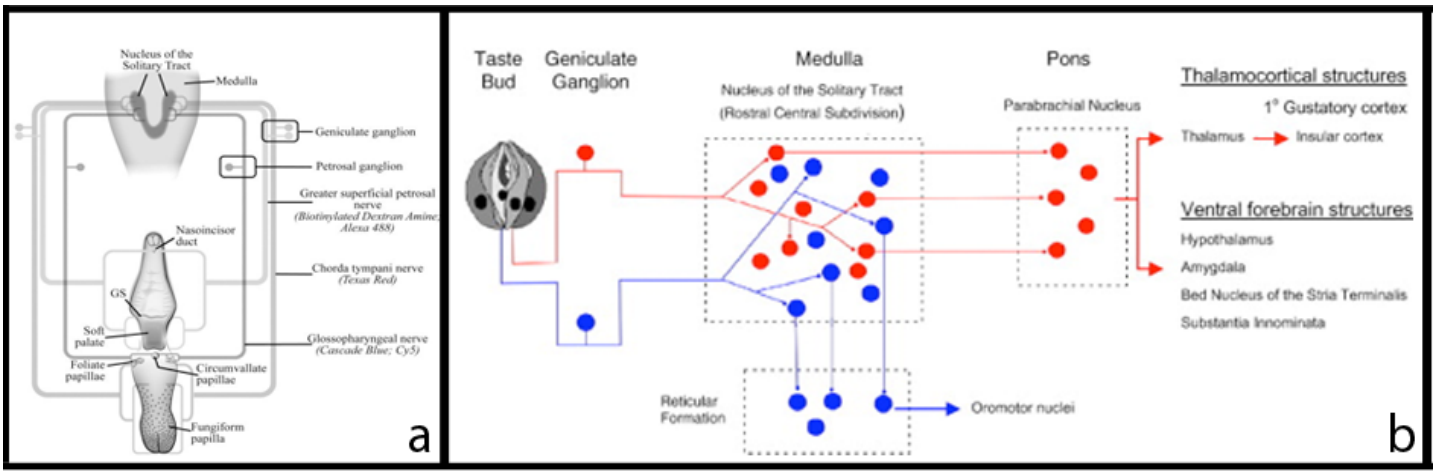

Figure 1: Gustatory information carried in the central nervous system of the rat follows a variety of pathways (a) From the fugiform papillae taste information is carried to the NTS via the CT nerve, while the circumvallate and foliate papillae have their gustatory information passed on via the CT and IXth nerves. The taste buds in the soft palate and nasoincisor duct, meanwhile, have information relayed by the GSP nerve (figure adapted from Mangold & Hill, 2008). (b) The pathways continue from the NTS in both and ascending and descending route, represented in this schematic. The ascending pathways are represented by the red neurons, which project from the NTS to the PBN, and then to the various other higher order centers. The descending pathway is represented by the blue neurons, which from the NTS project to the reticular formation and further oromotor nuclei. The schematic also suggests that these pathways operate in a parallel processing manner (figure obtained from Roper, 2009).

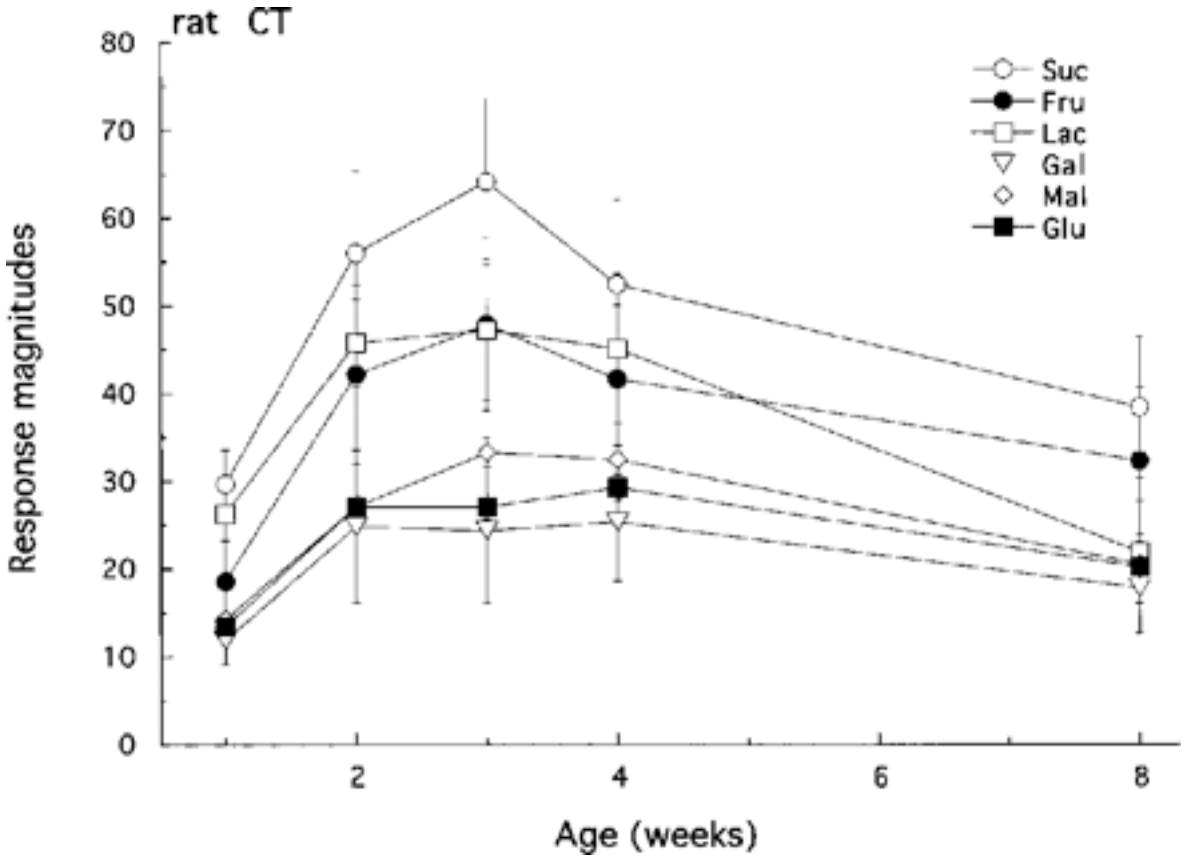

Figure 2:
Changes of the integrated electrophysiological response magnitudes of rat CT to six 0.5M sugars (sucrose, Suc; fructose, Fru; lactose, Lac; maltose, Mal; glucose, Glu; galactose Gal) (figure obtained from Harada & Maeda, 2004)

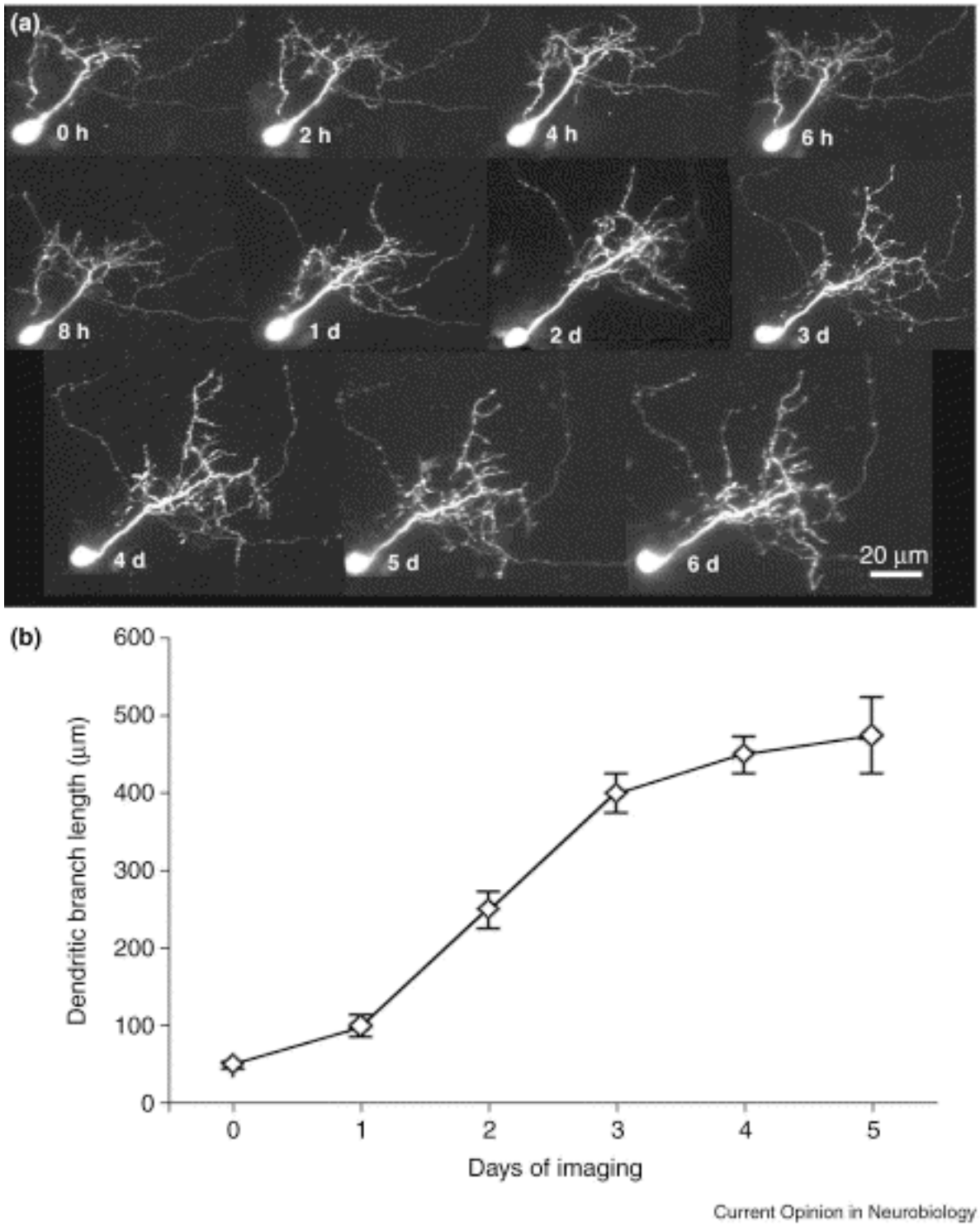

Figure 3:
In vivo dendritic arbor growth (a) *In vivo* images from *Xenopus* tadpoles of GFP-expressing optic tectal neuron across several days. (b) Rate of growth of the optic tectal neuron cell dendritic arbors (figure obtained from Cline, 2001)

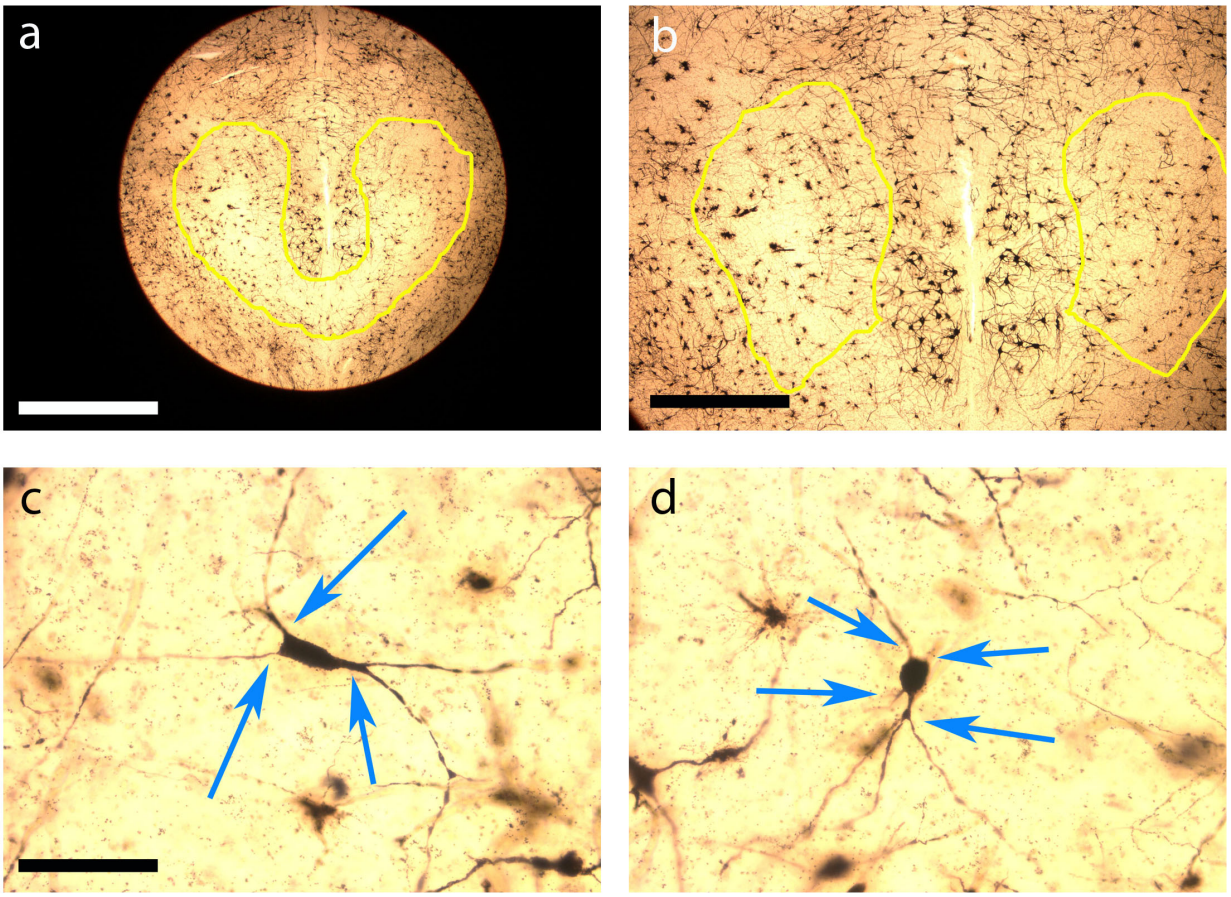

Figure 4
Neurons within the NTS can be categorized as either Class I or Class II, depending on their overt morphology and orientation within the nucleus. The NTS from a 49 day-old animal is shown and highlighted (a), with the rostral sections being the regions to which the IXth nerve projects to (b). Sample neurons are shown from the right (nerve cut) NTS side, with arrows indicating the location of dendritic bases. Class I neurons are more bipolar in shape, with longer dendrites that branch in a less complex fashion (c). Class II neurons have a more multipolar shape, with dendrites that branch more complexly and with greater frequency (d). Scale bar for Figure 4a is 2mm, scale bar for Figure 4b is 1mm, and scale bar for Figures 4c and 4d is 100µm.

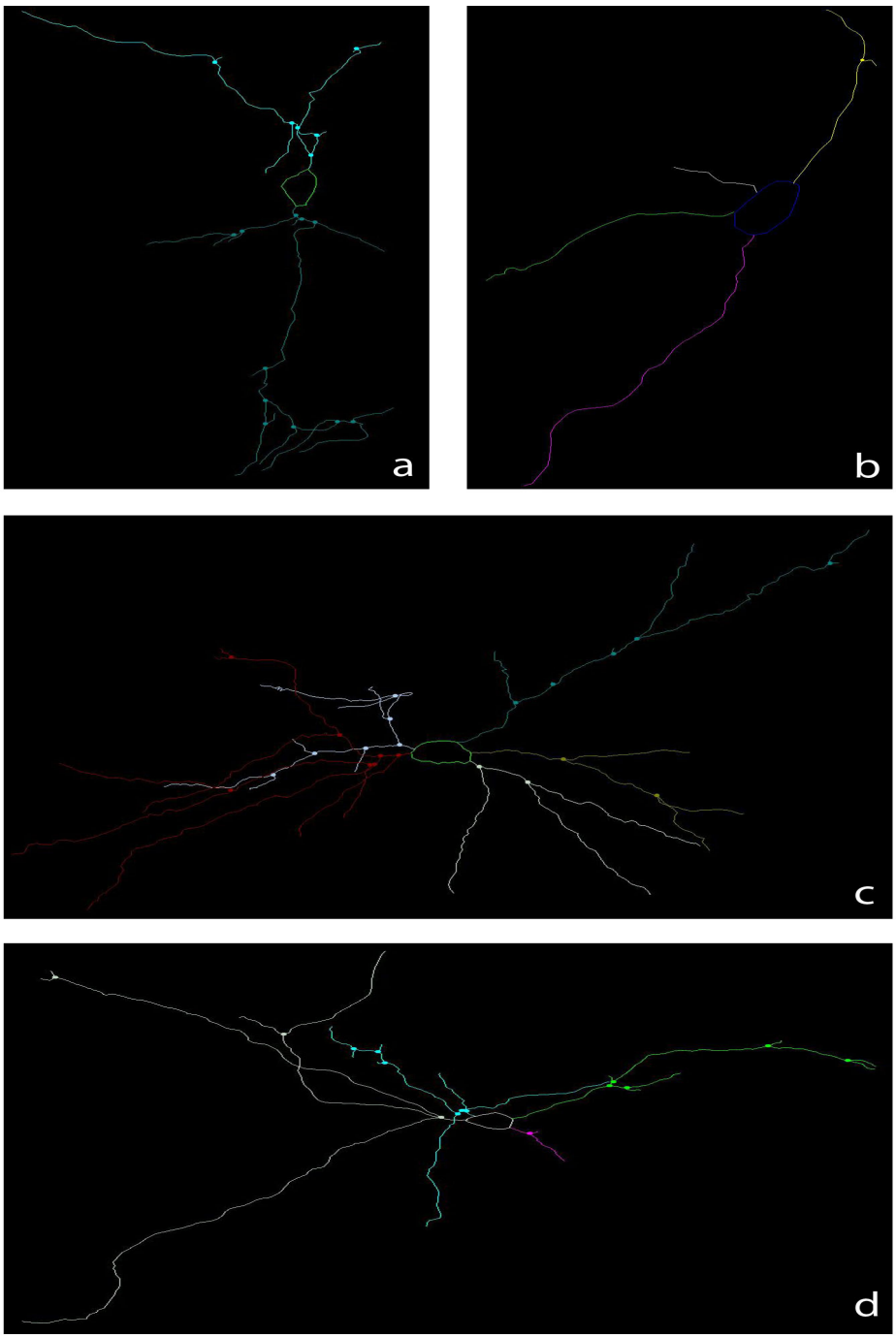

Figure 5
Neurolucida tracings reveal overt morphological differences between Class I and Class II neurons. Class I neurons (a, b) are characterized by fusiform shape and have fewer dendritic processes, which are less branched and cross less frequently than Class II neurons (c, d). Class II neurons have a more multipolar shape and have dendritic processes that are more highly branched. All representative tracings are taken from a 49 day-old animal, and all are shown at different magnifications as per normal Neurolucida display properties.

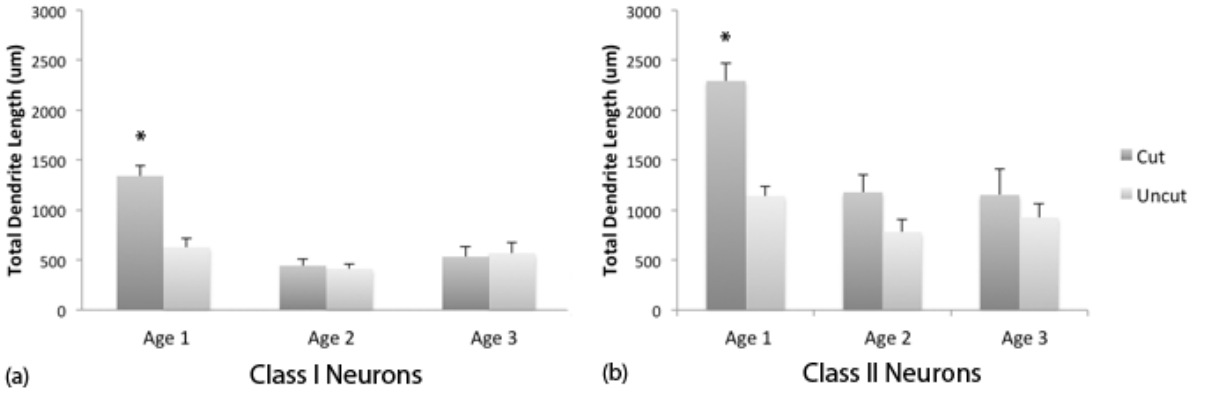

Figure 6
Plots of total dendritic length for each neuron reveal significant differences between the neurons in 49 day-old animals with cut IXth nerves compared to animals in all other groups. This effect is seen in both Class I and Class II neurons and a general trend of reduced total dendritic length between 49 day-old and 83 day-old animals is seen, followed by a slight recovery of total length between the 83 day-old and 114 day-old animals. Significance is shown at the $p < 0.001$ level, and Age 1 is 49 days-old, Age 2 is 83 days-old, and Age 3 is 114 days-old.

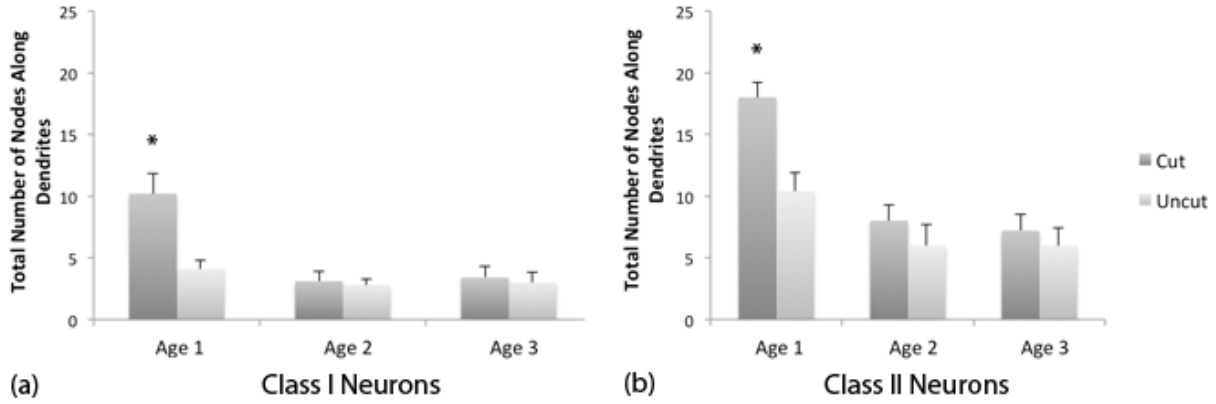

Figure 7
The total number of nodes per neuron show a similar pattern to the total dendritic lengths, with cut neurons in the 49 day-old age group showing a greater number of nodes in both neuronal classes. Significance is shown at the $p < 0.01$ levels, and Age 1 is 49 days-old, Age 2 is 83 days-old, and Age 3 is 114 days-old.

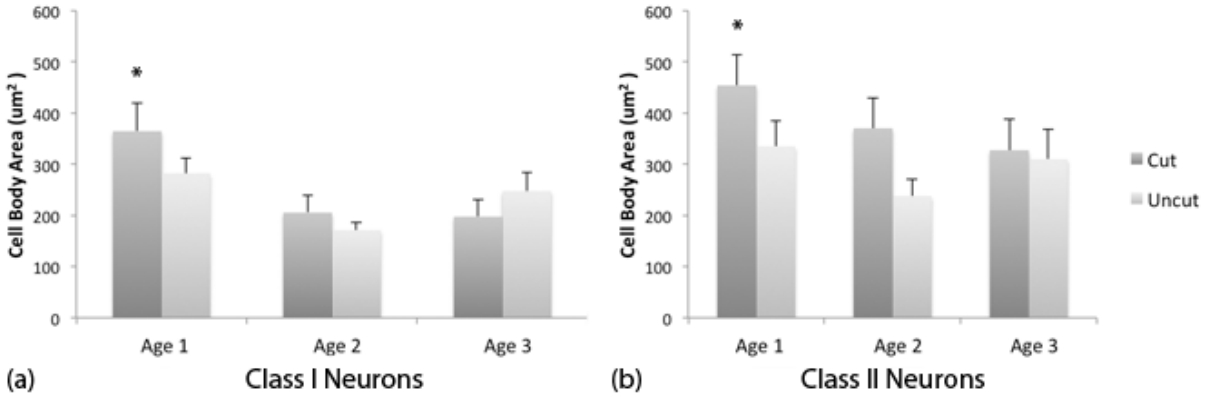

Figure 8
The cell body cross-sectional areas of cut condition neurons in the 49 day-old age group were significantly larger than all other groups for both Class I and Class II neurons, with the exception of uncut neurons in the same age group. While the differences were not as pronounced as they were for total dendritic branch length and total number of nodes, they were still significant at the $p < 0.05$ level. Age 1 is 49 days-old, Age 2 is 83 days-old, and Age 3 is 114 days-old.

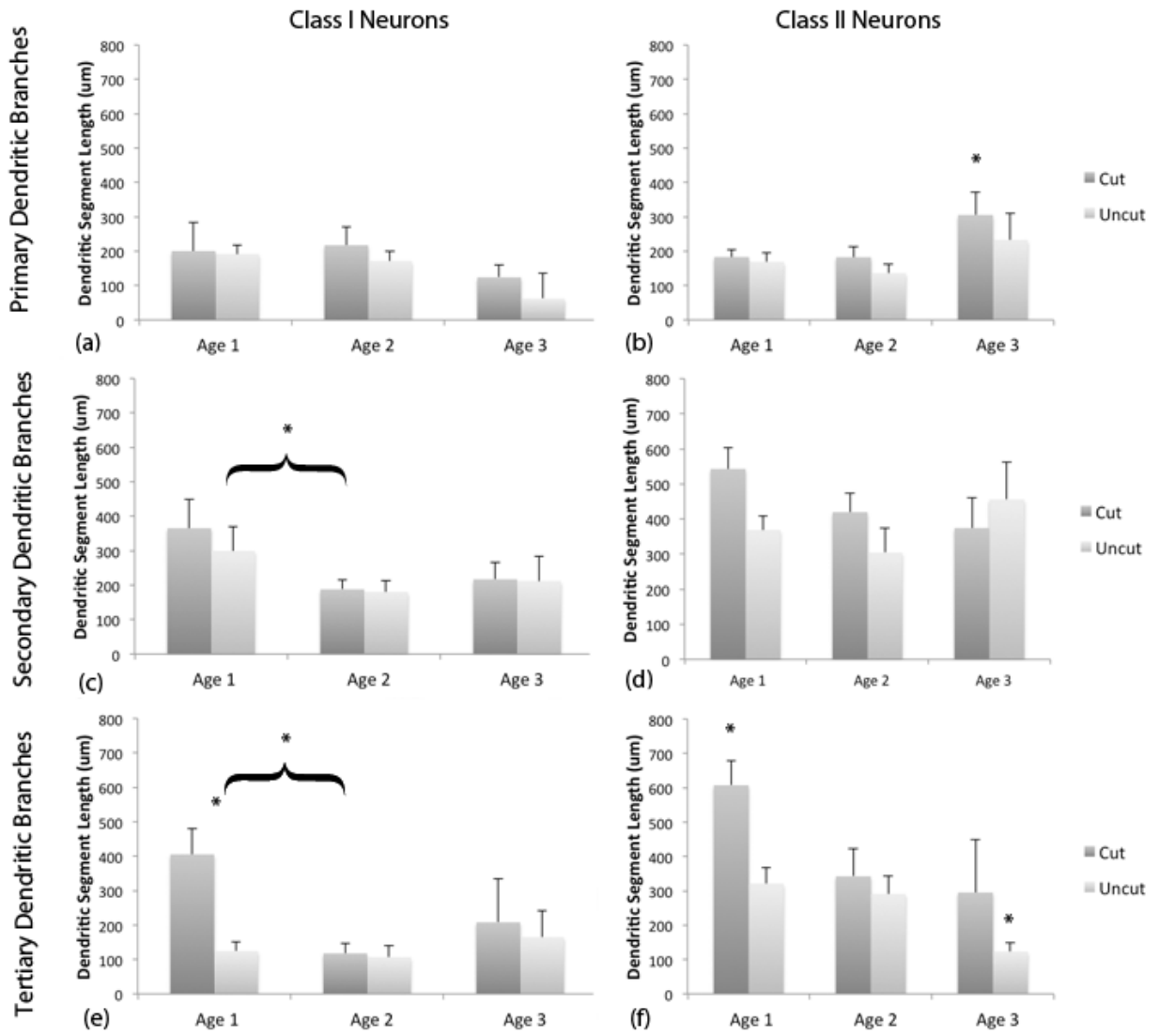

Figure 9

Among the specific branch segment lengths, tertiary dendritic branches most closely resemble the pattern of difference seen in total dendritic branch length. All significance is at the $p < 0.05$ level. The asterisk in 9b refers to cut condition neurons in the 114 day old animals having significantly larger primary dendritic segments than all the other groups, excepting uncut neurons in the same age group. The asterisk over the bracket in 9c refers to neurons in the 49 day-old animals – both cut and uncut conditions – having significantly longer secondary segments than neurons in the 83 day-old age group. The asterisk over the bracket in 9e refers to cut condition neurons in the 49 day-old age group having significantly longer tertiary segments than either the cut or uncut neurons in the 83 day-old age group. The asterisk not over brackets in 9e refers to cut condition neurons in the 49 day-old age group having significantly longer tertiary segments than uncut neurons in the same age group. The left asterisk in 9f refers to cut condition neurons in 49 day-old animals having significantly longer tertiary segments than cut or uncut neurons in any other age group. The right asterisk refers to uncut neurons in the 114 day-old animals having

significantly shorter tertiary branch lengths than any other neurons in all age groups, with the exception of cut neurons in the same age group. Age 1 is 49 days-old, Age 2 is 83 days-old, and Age 3 is 114 days-old.

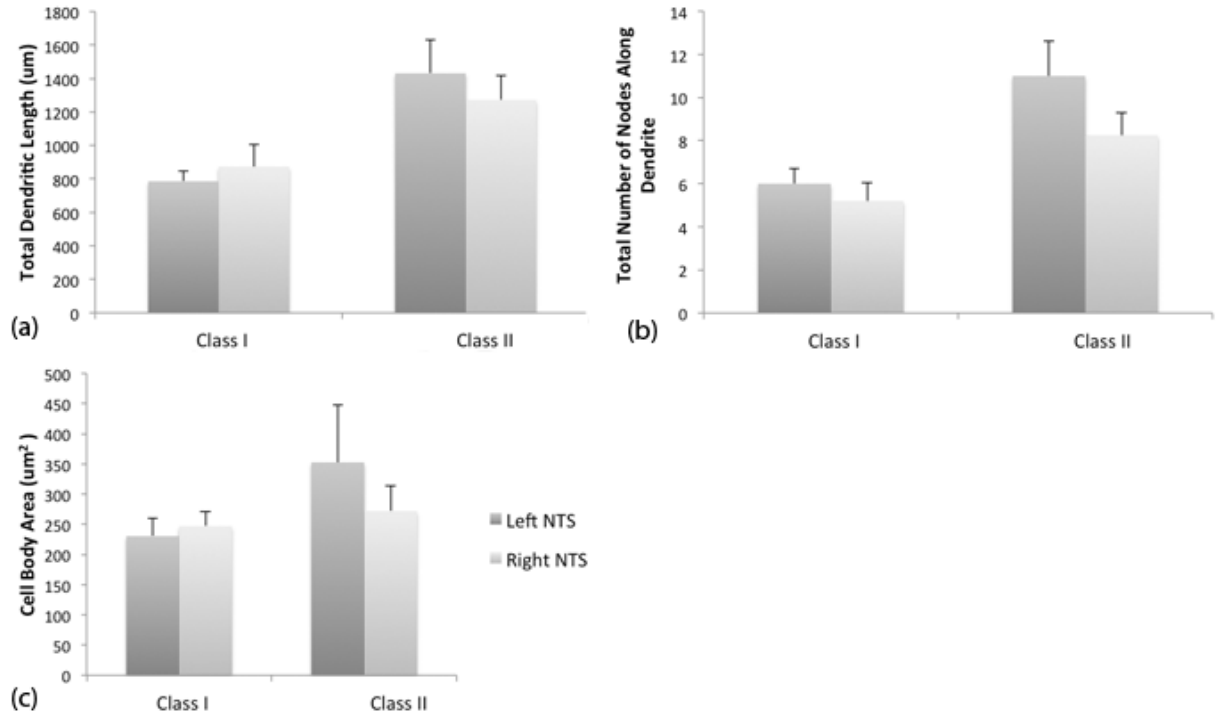

Figure 10
The total dendritic length (a), total number of nodes (b), and cell body size (c) were measured in a 49 day-old, sham surgery animal. Results indicate that there were no differences in neurons in left or right NTS – corresponding to what would be the uncut and cut sides, respectively, in a nerve cut animal – for any of the measured variables.

Class I		TDL (μm)	Standard Error	Total Nodes	Standard Error	Cell Body Area (μm^2)	Standard Error
Age 1	Cut	1340.5	105.9	10.2	1.6	364.7	54.9
	Uncut	627.4	87.7	4.1	0.7	282.3	30.6
Age 2	Cut	443.3	69	3.1	0.8	205.4	33.6
	Uncut	412.2	43.7	2.8	0.5	171.2	15.3
Age 3	Cut	533.5	96.8	3.4	0.9	197.6	33.6
	Uncut	568.6	104.1	3	0.8	247.8	36.4
Class II		TDL (μm)	Standard Error	Total Nodes	Standard Error	Cell Body Area (μm^2)	Standard Error
Age 1	Cut	2293	181	18	1.2	454.2	59.4
	Uncut	1141.4	100.1	10.4	1.5	335.1	49.1
Age 2	Cut	1178.6	173.9	8	1.3	370.4	58.7
	Uncut	780.8	126.8	6	1.7	238.2	32.5
Age 3	Cut	1152.5	259.8	7.2	1.3	327.5	60.3
	Uncut	926.3	136.4	6	1.4	309.9	59.3

Table 1
Means and standard errors for total dendrite length, total number of dendritic nodes, and cell body cross-sectional area in the experimental animals. TDL stands for Total Dendrite Length.

Class I		1° Length (μm)	Standard Error	2° Length (μm)	Standard Error	3° Length (μm)	Standard Error
Age 1	Cut	200.45	83.21	365.37	83.75	405.45	75.25
	Uncut	191.51	26.44	299.32	69.66	124.42	27.19
Age 2	Cut	217.3	53.77	187.88	27.44	117.88	29.45
	Uncut	171.37	28.72	180.32	32.5	106.74	32.51
Age 3	Cut	123.98	36.73	216.98	48.26	208	126.85
	Uncut	61.95	74.46	211.6	71.87	165.3	77
Class II		1° Length (μm)	Standard Error	2° Length (μm)	Standard Error	3° Length (μm)	Standard Error
Age 1	Cut	183.08	21.67	542.95	59.82	607.41	70.37
	Uncut	169.16	25.84	368.82	40.58	321.26	47.21
Age 2	Cut	182.5	30.71	419.83	53.84	342.32	80.82
	Uncut	136.37	25.51	304.27	70.97	290.98	52.18
Age 3	Cut	305.43	67.06	374.53	86.79	295.3	153.72
	Uncut	232.78	77.61	455.92	106.6	123.46	26.19

Table 2
Means and standard errors for the primary, secondary, and tertiary dendritic segment lengths in the experimental animals.

Class I		TDL (μm)	Standard Error	Total Nodes	Standard Error	Cell Body Area (μm^2)	Standard Error
	Left	786	59.1	6	0.71	230.5	29
	Right	874	130.8	5.2	0.84	247	24.3
Class II		TDL (μm)	Standard Error	Total Nodes	Standard Error	Cell Body Area (μm^2)	Standard Error
	Left	1431.3	200.3	11	1.63	352.7	95.1
	Right	1272.1	148.4	8.25	1.03	272.2	42.1

Table 3
Means and standard errors for total dendrite length, total number of dendritic nodes, and cell body cross-sectional area in the sham surgery animals. TDL stands for Total Dendrite Length.